Feasibility Study of a Balanced Upper Arm Orthosis based on Bending Beams

JL Stroo

Master of Science Thesis

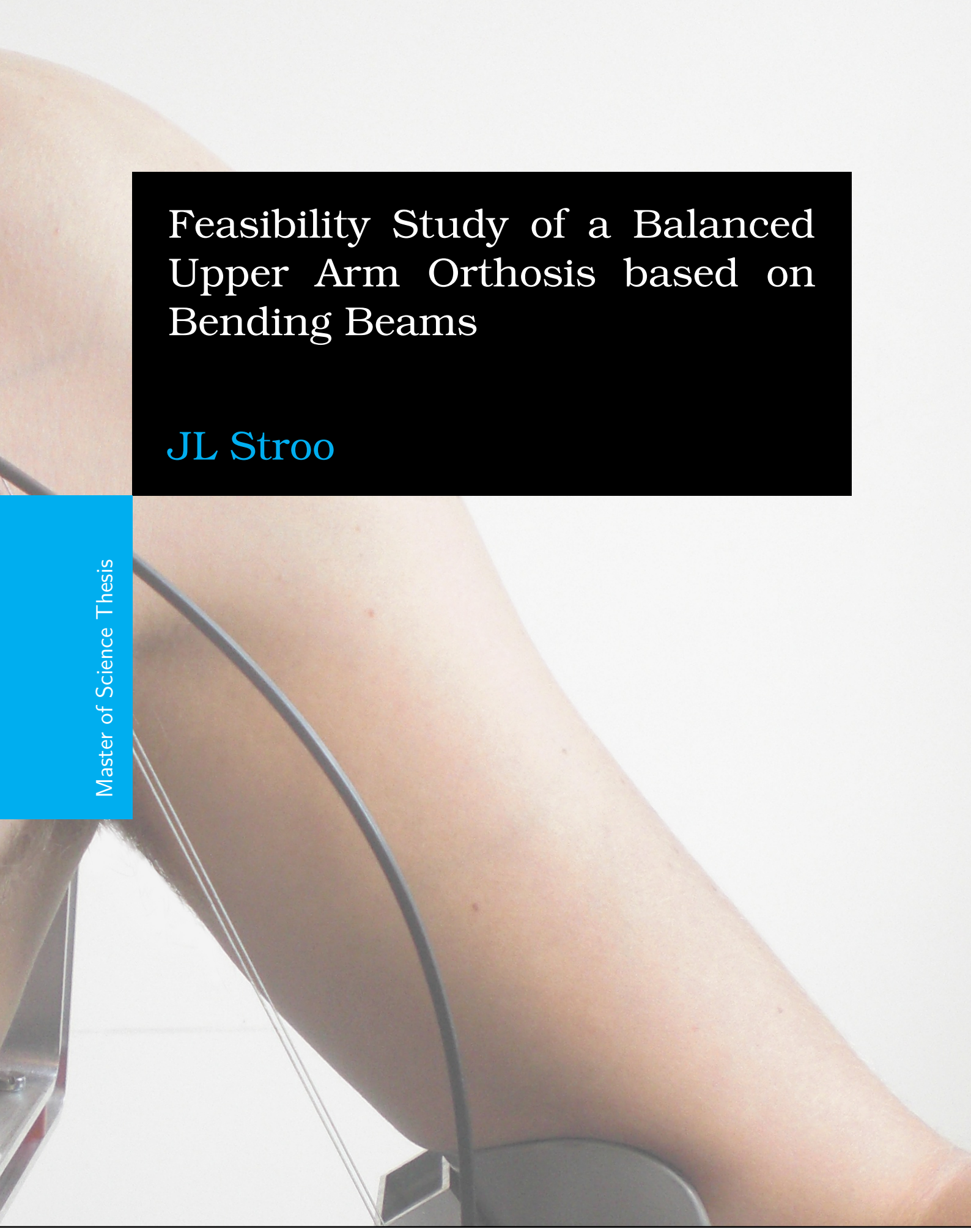

TU Delft Delft University of Technology

Interactive Mechanisms Research Group
Prof. dr. JL Herder
ir. AG Dunning

Feasibility Study of a Balanced Upper Arm Orthosis based on Bending Beams

Master of Science Thesis

For the degree of Master of Science in Biomedical Engineering at Delft University of Technology

JL Stroo

October 23, 2014

Faculty of Mechanical, Maritime and Materials Engineering (3mE) · Delft University of Technology

Preface

This thesis is the result of my graduation project for the master BioMedical Engineering. I wrote an article that proposes a design of an orthosis based on bending beams that assists arm movements. The appendices provide the background information of this article.

I fabricated a prototype, which was used for evaluation of the technical principle. A curiosity arose about how the concept would relate to the body in practice. Therefore I decided to make a second prototype which could be used on humans. It was very satisfying to make these prototypes and it was great that they worked the way it was, more or less, predicted.

I would like to thank all the people that helped me during my graduation project.

Contents

Feasibility Study of a Balanced Upper Arm Orthosis based on Bending Beams

JL Stroo[1], AG Dunning[1,2], G Radaelli[2], JL Herder[2]
Faculty of Mechanical, Maritime and Materials Engineering
[1]Department of Biomechanical Engineering, [2]Department of Precision and Microsystems Engineering
Delft University of Technology, The Netherlands
Email: A.G.Dunning@tudelft.nl

***Abstract*—People with neuromuscular diseases request an orthosis close to the body for assistance with their arm movements. This paper proposes a concept for a passive arm support that is close to the body and is based on bending beams. Simulations resulted in the final configuration and dimensions of the beams, optimised to balance an arm. One Carbon-fibre-reinforced polymer beam with dimensions 0.22x0.0041x0.0027m at the medial side and one at the lateral side of the upper arm delivers the required energy for balancing the arm. Experimental evaluation of a prototype demonstrated the technical principle; more than 87% of the moment around the shoulder was balanced between 0 and 1.1rad. A second prototype was built for preliminary evaluation of the concept in relation to the body. The width of the elastic and structural elements was more than four times smaller than in present arm supports. From this it was concluded that bending beams have the potential to make an orthosis that is closer to the upper arm than current orthoses.**

***Index Terms*—Arm support; static balancing; inconspicuous; beams; assistive device; orthosis; wearable;**

I. Introduction

PEOPLE with neuromuscular disorders (e.g. Duchenne Muscular Dystrophy (DMD)) often have muscle weaknesses and therefore are dependent on assistive devices to perform activities such as picking up objects and eating. DMD is one of the most common dystrophies, affecting around 1 in 3500 male births [1]. The main symptom is progressive degeneration of the muscles, beginning with the largest and most proximal muscles (upper arms, shoulders, upper legs). Around the age of ten the patients end up in a wheelchair because of the deterioration of the upper leg muscles. In the years as teenagers, they can no longer lift their arms against gravity due to a lack of muscle strength. Providing these patients with assistive devices enable them to use their arms again.

The goal is to propose a concept for an orthosis that fits within 20mm from the body. It is important that these devices are close to the body, because the patients prefer a support that is unobtrusive and consequently not stigmatising [2]. However, the orthosis that is closest to the upper arm (WREX, Jaeco Orthopedic, USA), according to the knowledge of the authors, is approximately at a distance of 65mm. This is too large to be inconspicuous and therefore does not meet the demands of the patients.

Dunning [3] compared 23 arm supports and concluded that the active (powered) orthoses had, on average, a larger volume than the passive (non-powered) orthoses. This was mainly due to the actuators that were situated locally at the joints or at a large structure on the back. The focus of this project will be on a passive device, because without actuators the orthoses have the potential to be located closer to the body.

(a) ARMON

(b) WREX

Figure 1: (a) An arm assisting aid [7] that is not in proximity to the body due to the linkage that connect the fore-arm support to the wheelchair. (b) In this design (WREX) links are required to convert the pulling force of the springs (red rubber bands) to a supporting force on the arm.

The orthosis is intended for assistance during a large range of upper arm movements. In the first place the design is concentrated at the support during eating movements, because that is considered as one of the most essential activities to perform independently for people with DMD [4][5][6].

Two strategies have been implemented to make the device smaller than the current orthoses. The first strategy is to focus on a device that has the same kinematic structure as the arm. The majority of the existing passive orthoses use a linkage from the wheelchair to the forearm (Fig. 1a). With such structure, the device configures to the best position,

which can lead to links positioned far from the body. This might be avoided by the design of a device that moves alongside the arm.

The second strategy is to use a balancing mechanism with bending beams instead of springs. In the existing passive orthoses the arm is statically balanced with spring mechanisms. The springs that are currently used mainly comprise helical springs and rubber bands [3]. These springs can only exert a pulling force and therefore a linkage is required that converts the pulling force of the springs to a supporting force on the arm (Fig. 1b). Beams can exert both a pushing and a pulling force, and consequently no links are needed for connection to the arm.

This paper starts with introducing the requirements for balancing the arm. It is followed by explanation of the balancing principle with beams and simulations of the conceptual design. The beams were dimensioned to balance an arm and experimental evaluation of a prototype proved the technical principle. A second prototype was built to evaluate the concept in relation to the arm. The paper finalises with discussion of the prototypes, followed by some concluding remarks.

II. Analysis

A. Representation arm

Fig. 2 shows the representation of the arm. The angle is 0rad for the arm vertically pointing down and increases to 1.57rad for a horizontal arm. The shoulder joint is represented with a fixed rotation point (IC). The mass of the forearm and hand is simplified to act as a point mass on the elbow. Combined with the mass of the upper arm, based on anthropomorphic data of Winter [9], this results in a 3.84kg mass with a CoM at 0.23m from the centre of the glenohumeral joint.

B. Requirements

The following requirements resulted from interviews with experts and literature search:

- Inconspicuous: The orthosis must fit within 20mm from the body, to fit underneath clothing and be unobtrusive.
- Comfortable: A condition for comfort is that the shear force on the skin should be kept very low. The functioning of the sweat gland should not be obstructed, so no pressure on the axilla is allowed.
- Support: The device should compensate approximately 90% of the moment that is required to lift the arm.
- Eating movement: The range of elevation required for an eating movement (0 - 1.1rad [8]) must be facilitated by the device.

It is assumed that the device can be rigidly connected to the trunk by a corset, that is often worn by people with DMD for stabilising the trunk.

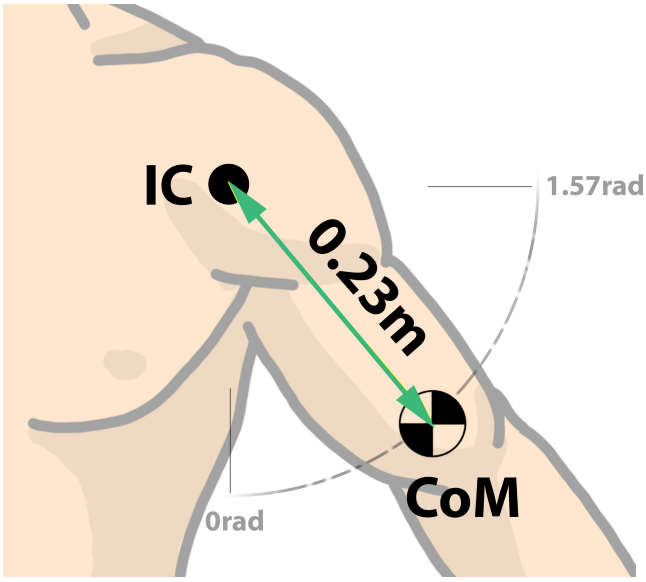

Figure 2: Representation of the arm. The arm is represented as a point mass with a Centre of Mass (CoM) at 0.23m from the Instantaneous Centre (IC). In this figure the frontal plane is the plane of elevation, for clarity of the illustration, but this can be any plane that is convenient for eating.

C. Goal Function

The goal function is the characteristic of the required energy to passively balance the arm. The energy stored in the device should approximate the goal function for balancing the upper arm.

The potential energy of the arm increases during elevation. This increase in energy should be provided by a release of energy in the device. During lowering of the arm the energy should be restored in the device. Fig. 3 shows the potential energy of the arm and the energy that the device should contain to balance the arm (the goal function). If this goal function is met, the arm is 100% balanced. The focus will be on the elevation until 1.1rad, because that is the maximum angle during eating [8]. The arm can be considered as a point mass because the inertia does not have a substantial influence on the moment that is required to balance the arm during eating.

III. Conceptual design

A. Beams as a method for storing energy

The most promising principle for storing elastic energy is selected according to the following method to use in the device for balancing the arm. The principles are revealed by categorising them by deformation mode and dimension of the principle. Eight options that resulted from this classification are compared regarding the requirements. Storing elastic energy in beams turned out to be most favourable because the beams can function both as the structure and as the elements for energy storage. With this principle no separate links are needed for the structure and therefore it has the potential to result in a device close to the body.

Beams can be straight in unstressed state or curved in unstressed state. A curvature in the beam can change the

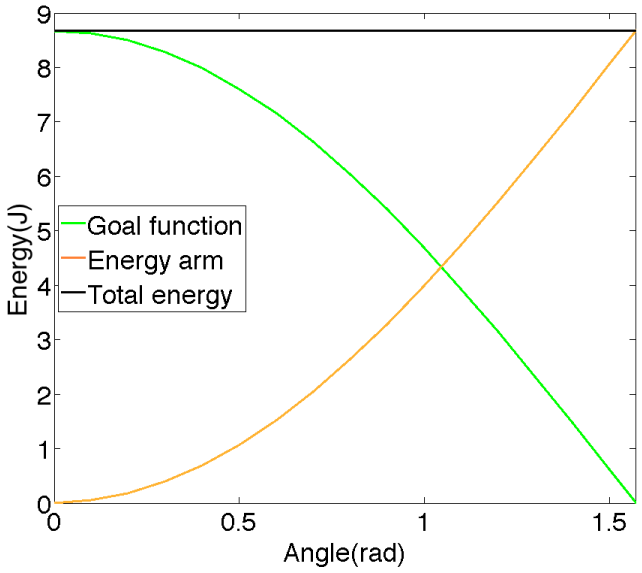

Figure 3: The energy-angle characteristic of the goal function, the arm and the sum of these characteristics. The arm will be balanced if the energy stored in the device approximates the goal function.

behaviour to the desired performance, as Radaelli et al. [10] showed with a curved beam balancing a pendulum. However, this project focuses on balancing with beams that are straight while unstressed, because these beams have advantages with respect to analysis and manufacturability.

B. Final concept

Fig. 4 shows the configuration of the final concept in relation to the arm. The instantaneous centre (IC) is fixed around the location of the shoulder joint. One end (B1) of a simply supported beam is vertically placed under IC. The other end (B2) connects to the arm. A cable connects B2 to IC and constraints the movement of B2 only to rotation around IC. The resultant of the force in the cable directed to IC (F_{IC}) and the force in the beam (F_{B1B2}) is a force perpendicular to the arm. This force (F_{Supp}) generates the balancing moment around the shoulder joint.

IV. Simulation

Isogeometric Analysis [11] was used for simulation of bending beams. The purpose of the simulation was to find a beam configuration of which the energy-angle characteristic approximates the goal function.

A. Isogeometric beam formulation

The unstressed position of the beam is defined with four control points that describe a third order non-uniform rational B-spline (NURBS) curve [12]. The control points are positioned equally spaced on one line, with an offset on the two inner points of $0.001 * lengthbeam$ from the line. This offset prevents singularity during bending of the beam. The curve is refined with 10 control points to increase the flexibility of the curve.

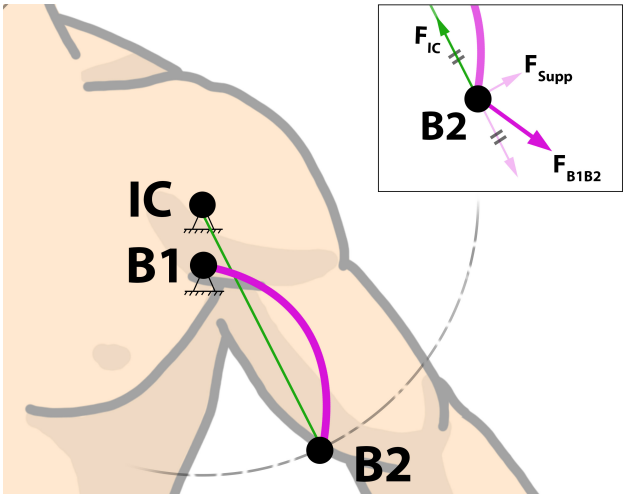

Figure 4: The final concept for balancing the arm. A simply supported beam is fixed on one end (B1) to the trunk and on the other end (B2) to the arm.The resultant of F_{IC} and F_{B1B2} is a supporting force perpendicular to the arm (F_{Supp}). This force balances the arm by generating a moment around the shoulder joint.

B. Constraints

The augmented Lagrangian method is used for addition of the constraint equations to the stiffness equations. The position constraints on the endpoints (B1 and B2) are applied with the following equations:

$$\begin{bmatrix} 1 & 0 & 0 & 0 \\ 0 & 1 & 0 & 0 \\ 0 & 0 & 1 & 0 \\ 0 & 0 & 0 & 1 \end{bmatrix} * \begin{bmatrix} X_{B1} \\ Y_{B1} \\ X_{B2} \\ X_{B2} \end{bmatrix} = \begin{bmatrix} 0 \\ 0 \\ cos(\alpha) \\ sin(\alpha) \end{bmatrix} \quad (1)$$

were the right vector represents the constraints on the endpoints and the left vector represents the actual position of the endpoints. B1 is fixed at position (0,0) and B2 is constrained to a circular arch. α starts at 1.5π and increases in 40 steps to 2π.

C. Shape of beam

The system of equations is solved with a displacement control algorithm for nonlinear solutions. The solution consists of the reaction forces at the endpoints and the displacement of all other control points. The position of the control points defines the shape of the beam in stressed position.

D. Energy in beam

The elastic strain energy (U) of planar Bernoulli-Euler beams is given as:

$$U = \int [EA(\lambda - \lambda_0)]^2 + EI(\kappa - \kappa_0)^2] dS \quad (2)$$

where E, A, I, dS represent the elastic modulus, the cross-sectional area, the area moment of inertia and the initial differential beam length respectively [13]. E, A and I are considered constant over the whole beam length. λ is the stretch and κ the curvature of the neutral axis which are defined by the shape of the beam.

IC-B1 (m)	Deviation (Nm)	Max dev. (Nm)	Max F_{IC} (N)	Thickness	Width (m)
0.0125	1.64	0.13	351	0.0043	0.0023
0.025	2.31	0.20	173	0.0027	0.0040
0.05	4.98	0.43	86	0.0018	0.0068

Table I: The influence of distance IC-B1 on parameters of the design. The width of the beams can be smaller and the goal function is better approximated if IC-B1 is smaller.

The integral of equation 2 is approximated with a Gaussion quadrature rule which is evaluated to obtain the energy in the beam.

E. Approximation of goal function

Fig. 5a shows the relation between the energy in a simply supported beam and the distance between the end-points B1 and B2. B1B2* represents the distance between B1 and B2 in unstressed position of the beam. B2 vertically translates until the distance is 0.9 times B1B2*. The goal function is approximated if a sinus shaped geometric relation exist between 'elevation of B2' and 'distance between B1 and B2'. This is achieved if B2 follows a trajectory with IC as instantaneous centre while B1 is placed under IC (Fig. 5b).

The combination of the relations 'distance B1-B2 – Energy' (Fig. 5a) and 'Elevation – distance B1-B2 (Fig. 5b) leads to the relation between elevation and energy (Fig. 5c). The energy of the beam approximates the sinusoidal goal function for balancing the arm.

V. Dimensional design

The final concept is dimensioned to store enough energy to balance the arm until 1.1rad.

A. Influence of variables on energy in the beam

The cross-sectional area A in equation 2 is $w * h$ and the area moment of inertia I is $w * h^3/12$, where w an h represent the width and thickness, respectively. This implicates that the energy in the beam linearly relates to the width of the beam. The thickness of the beam is to the third power related to the energy in the beam.

The relation between the distance IC-B1 and the energy in the beam is more complex, because the distance IC-B1 influences several parameters including the curvature of the beam. To illustrate the effect of the distance, beams are considered that are straight at 1.1rad and contain a max of 1% strain. Table I shows the influence of IC-B1 on the deviation of the moment of the device from the moment required to balance the arm for 100%. It further states the influence on F_{IC}, length, thickness and width of the beam. Advantages of a smaller distance IC-B1 are a smaller deviation from the goal function and a smaller width. The disadvantages are a larger force F_{IC} and larger thickness.

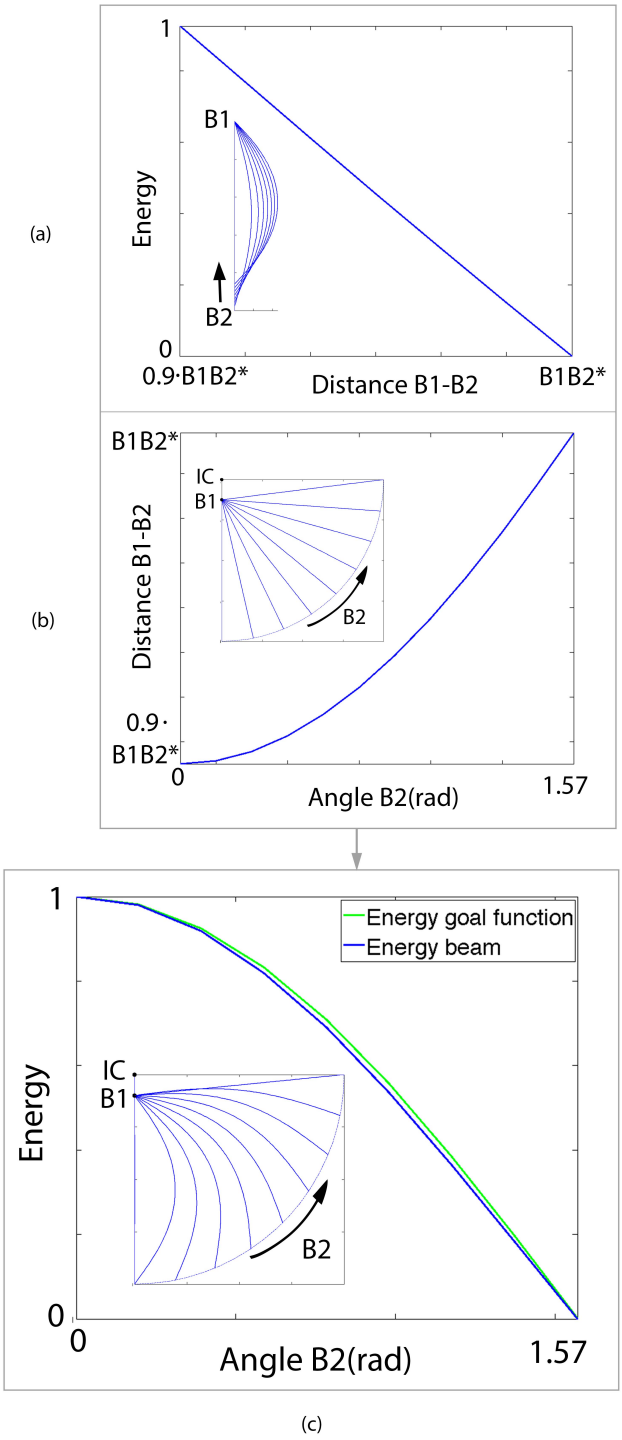

Figure 5: (a)The relation between the 'distance B1-B2' and 'energy in the beam'. (b)The relation between 'elevation of B2' around an instanteneous center (IC) and the 'distance B1-B2'. (c)The relation between the 'elevation of B2' and the 'energy in the beam', which shows that the energy in the beam during elevation is close to the goal function.

Material	Unidirectional CFRP (50% fibre)
Elastic modulus	121GPa [14]
Tensile strength	2450MPa [14]
Distance T-S	0.025m
Number of beams	2
Length	0.22m
Width	4.1mm
Thickness	2.7mm

Table II: Properties of the dimensioned design.

B. Material

An orthosis close to the body requires beams that can store a large amount of energy while having a limited width. Carbon-fibre-reinforced polymer (CFRP) is chosen as material for the beams because of the high elastic energy storage-to-width ratio during bending.

C. Final dimensions

Table II shows the material properties and the dimensions of the beams in the final design. Distance IC-B1 is defined as 0.025m, considering the trade-off between matching the goal function, the volume of the beam and the force F_{IC}. One CFRP beam with width 4.1mm and thickness 2.7mm at both sides of the arm stores sufficient energy to produce the required support.

VI. Prototype #1

A. Prototype description

Fig. 6 shows the prototype that is built for experimental evaluation of the balancing principle. A rectangular shaped piece of wood (0.27x0.06x0.08m, 0.54kg) represents the arm. A socket facilitates the suspension of the armarm. The arm is kept in place by a rod (representing the "shoulder joint") through the arm and socket. A second rod is inserted at 0.20m distance from the first rod. The notches in this rod keeps the beams in place. The other side of the beams are attached to a notch in a screw, through the socket, 0.025m under the first rod. The beams are made of carbon-steel with dimensions 0.202x0.049x0.008m and support the arm with a range of motion from 0 to 1.57rad.

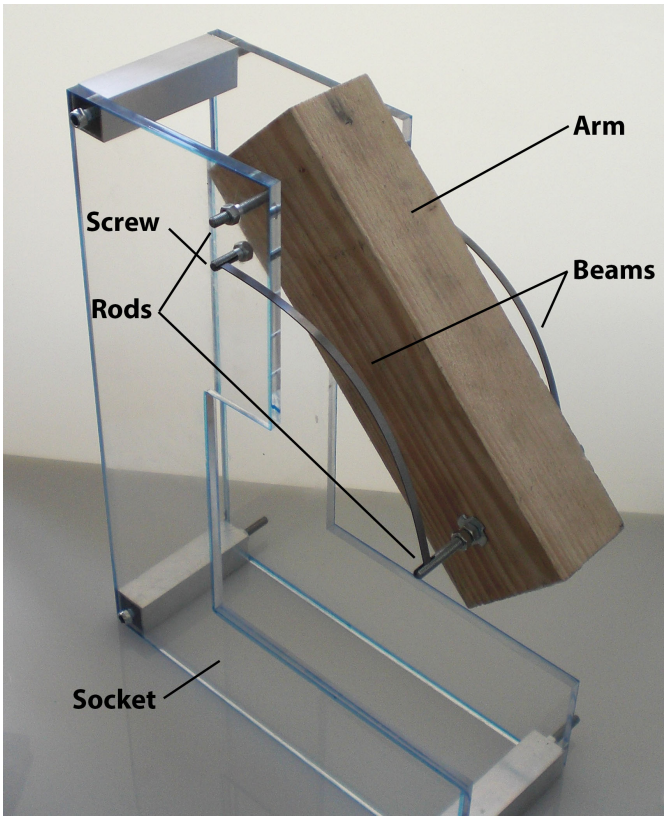

Figure 6: Photograph of prototype #1 for evaluation of the support of the beams.

B. Simulation

Fig. 7 shows the moment that, according to the simulations, is balanced with the beams in prototype #1. Two of these beams (one at the front and one at the back) result in a support of 84% at 1.1rad. This can be increased to a support of 100% at 1.1rad if the beams store 19% more energy (dashed line in Fig. 7).

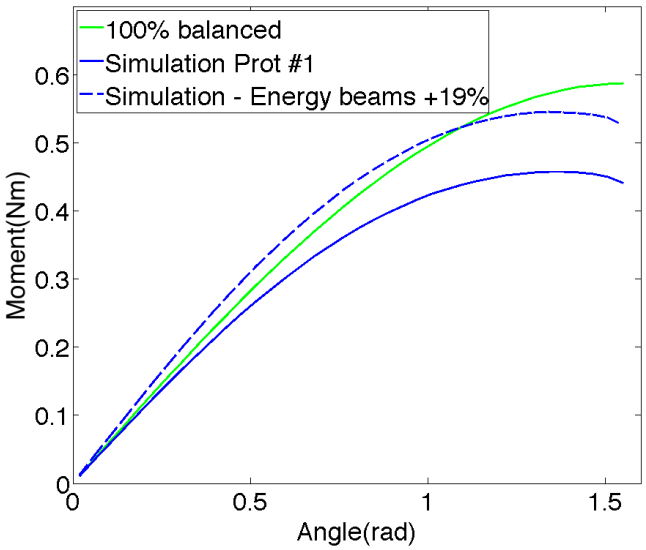

Figure 7: The beams on prototype #1 balance 84% of the moment around IC at 1.1rad. The balancing at 1.1rad can be improved to 100% if the energy in the beams is increased with 19% (dashed line).

C. Experimental evaluation

A setup was built to measure the moment required to balance the arm with and without beams. This section describes the measurement setup, the measurement protocol and the results of the measurements.

1) Measurement setup: The setup built for experimental evaluation of prototype #1 is shown in Fig. 8. A rotation was applied on the arm and the force was measured.

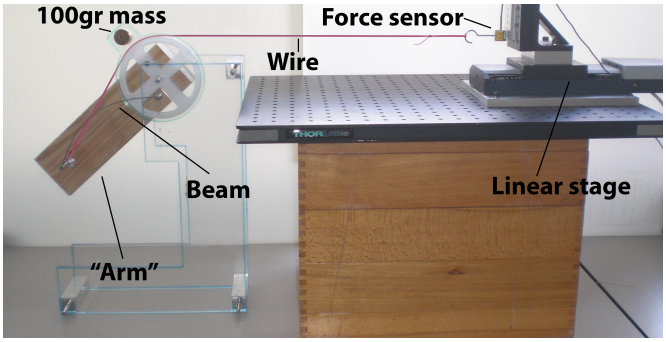

Figure 8: The setup for evaluation of the moment that is balanced by prototype #1.

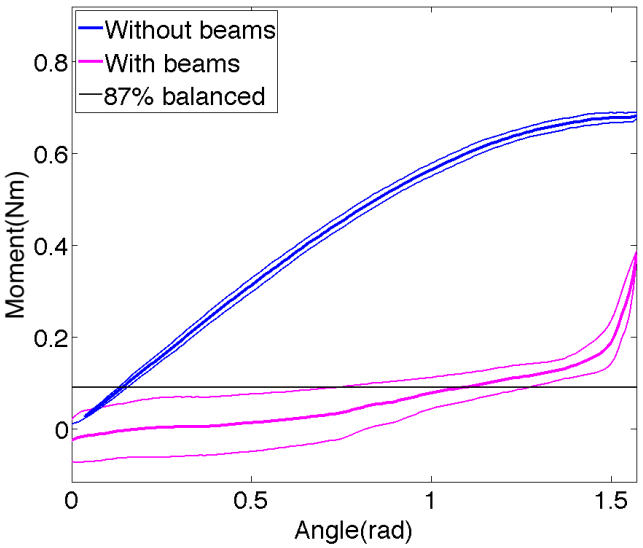

Figure 9: Hysteresis loops (thin lines) of the moment-angle characteristic of prototype #1 measured with and without beams. If the average (thick lines) of the up and down movement is taken as the remaining balancing moment, more than 87% of the moment of the arm is balanced by the beams until 1.1rad.

A wire ran over a pulley and connected the prototype to a force sensor (FUTEK LSB200, resolution: 10mV, range: 0-44.5N). The displacement was performed and measured by a linear motor stage (Physik Instrumente M-505.4DG, resolution: 0.05 µm, travel range: 107mm), connected to a wire through the force sensor. The data was read using an amplifier (ICP DAS 3016) and a data acquisition module (National Instruments USB6008). The data was logged with the software Labview 12 and processed with MATLAB R2014a. A 100gr weight was attached to the pulley for assuring a pulling force on the force sensor. The effect during elevation of the 100gr weight, a sinus shaped moment, was subtracted from the total moment during processing of the measurements.

2) Measurement protocol: In the first experiment the beams were attached to the prototype. The arm was rotated from 0 to 1.57 rad by movement of the linear stage. After the arm was rotated 1.57rad, the linear stage moved the opposite direction and returned the arm to its start position for measuring hysteresis effects. In the second experiment the beams were removed and the measurement was repeated.

3) Results: In Fig. 9 the moment-angle characteristic of the arm with and without beams is shown. The thick pink line represent the average of the up and down movement with beams attached to the arm. This is approximately the remaining moment that balances the arm if the friction is neglected. The thick line of the prototype with beams intersects with the horizontal line, which represents 87% balancing quality, at 1.1 rad. This means that until 1.1 rad 87% of the moment of the arm is balanced by the beams. In the simulation 84% of the moment was balanced, this approaches the 87% of the measurements.

In Fig. 10 the results of the moment-angle characteristic of the beams for both the simulation and the measurements are shown. Until 1.4rad the characteristics have large similarities, but for larger angles the measured moment declines much steeper than can be expected from the simulations.

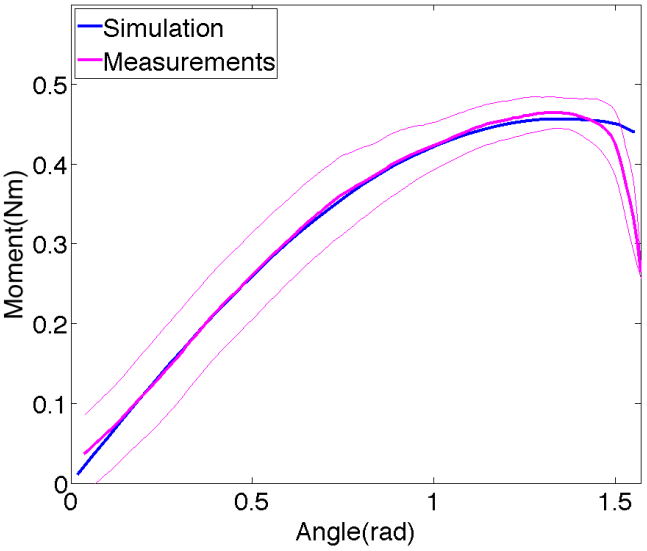

Figure 10: The moment-angle characteristic of the beams with simulation (blue) and measurements (pink). Until 1.4rad the simulation is a good predictor for the moment that the beams exert on the arm during the experiments.

VII. Prototype #2

A. Prototype description

Fig. 11 shows the prototype that was built for evaluating the proximity to the arm and the comfort of the device. A beam is connected to a U-shaped structure at the front by a slide bearing. The structure is connected to the seating and assures a fixed rotation point at the front and at the back of the shoulder. A steel wire is connected to point IC by a rod that is fixed on the structure. At the back side the structure connects to a second beam and wire. Both wires and beams are connected to a cup that transfers the supporting force to the upper arm. The beams have dimensions 0.23x0.0025x0.0025m and are made of unidirectional carbon-fibre-reinforced polymer.

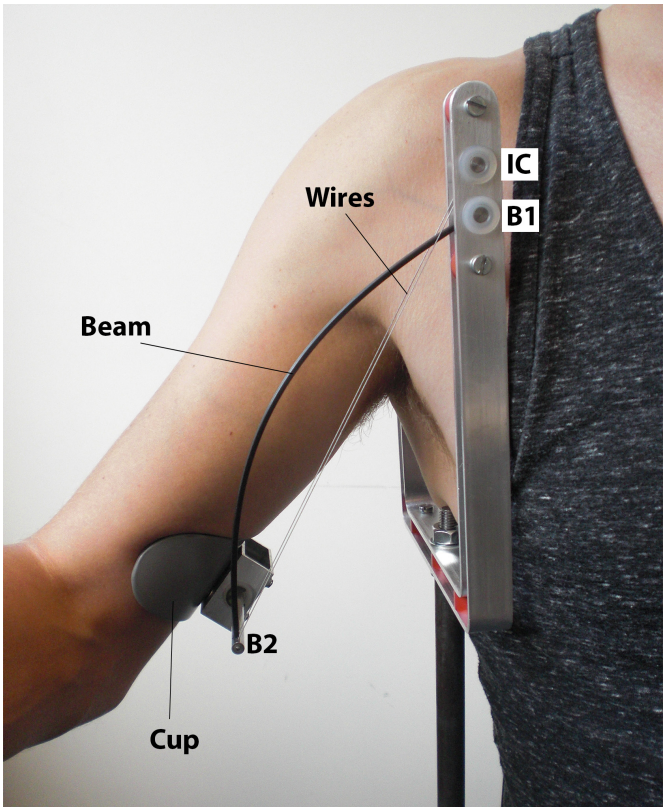

Figure 11: Prototype #2 in relation to the arm. The beams and wires are connected on one end to a cup that supports the arm. The other ends are connected to a U-shaped profile that facilitates the fixed rotation points at the front and the back of the shoulder.

B. Experimental evaluation

1) Measurement protocol: Measurements with prototype #2 were done to analyse the proximity to the arm and the shear forces on the arm. The distance from the arm to the outer point of the device was measured with a caliper.

The shear force between the cup and the skin of the upper arm was indicated by the movement of the skin with respect to the upper arm during elevation. The position of the cup was marked in start position (0 rad) and in end position (1.1 rad), whereafter the distance between the two marks was recorded.

2) Results: The maximum distance of the device to the arm is 59mm (Fig. 12). The width of the combination of beam and wires is 7.5mm. No movement of the cup with respect to the skin was observed during elevation of the arm. The mass of the orthosis (without fixation to chair) is 0.11kg.

VIII. Discussion

A. Conceptual design

It must be noted that the mass of the hand and arm was simplified to act as a point mass on the elbow. A future design should be extended to the fore arm, to incorporate balancing of the moment of the fore arm on the upper arm.

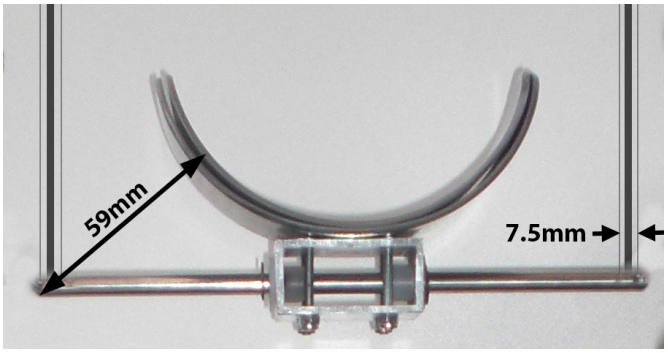

Figure 12: Front view of the cup in relation to beams, wires and structure in between. The maximum distance from the arm to prototype #2 is 59 mm, the width of the beam and wires is 7.5mm.

In the first place the focus was on the eating movement, but during further research the concept has to be extended to assist during other important daily activities. It was noticed that the arm of prototype # 1 can be balanced if a beam was connected to only one side of the socket. If this principle can be integrated in an orthosis, with only a connection at the front of the shoulder, the patient might benefit from an increased range of motion.

B. Prototype #1

The carbon steel beams balanced the arm for 87% at 1.1rad. This can be raised to 100% at 1.1rad if the beams can store 13% more energy, for example by using beams that are 0.03mm thicker ($0.03{=}h * \sqrt[3]{1.13}$).

Theoretically the moment slightly decreases after 1.3rad and goes discontinue to zero when the unstressed shape is reached at 1.57rad. In practice, the moment decreases much steeper after 1.3rad. A slight curve of the beams in unstressed state was observed after the experiments. Fig. 13 shows that a pre-formed curvature can explain the decrease of moment after 1.3rad. The plastic deformation could be prevented by using a material that has a higher elastic strain limit, for example spring steel.

The experiment with beams showed a larger hysteresis loop than the experiment without beams. This could be explained by the increased forces on the sliding surfaces between the beams, screws, rods and socket, which add friction to the system (Fig. 14). The size of the hysteresis loop decreases for larger angles, which has similarities to the reduced force on the joints for larger angles. The friction in this prototype could be reduced by the use of bearings.

C. Prototype #2

During elevation of the arm, no displacement between the skin of the arm and the device was observed. This suggests that the shear forces were low. Even with a 20-30mm deviation of IC from the point of rotation at the shoulder joint the cup did not move with respect to the skin. This suggests that IC is not required to be accurately positioned in order to have low shear forces.

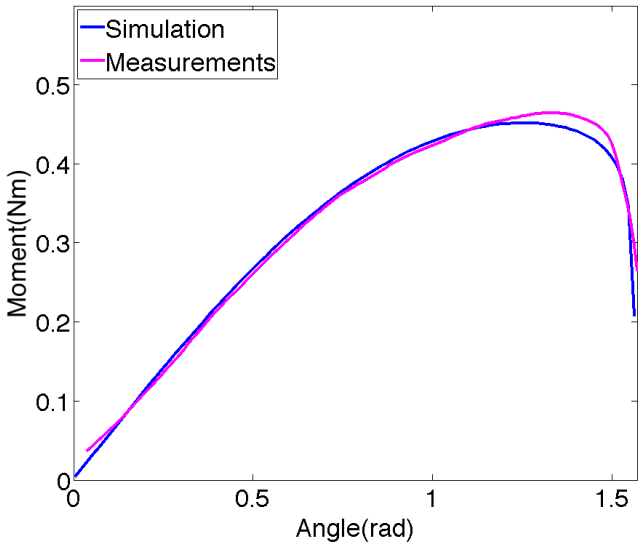

Figure 13: The simulation with a curved beam (thick blue line) shows that the decrease after 1.3rad could be devoted to the pre-formed curvature.

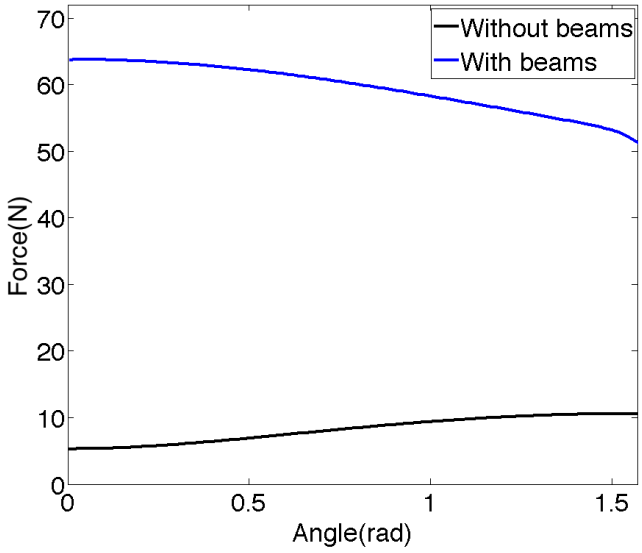

Figure 14: Sum of the force on the joints of prototype #1 with and without beams inserted. The larger hysteresis loop of the experiments with beams (Fig. 9) is attributed to the increased force on the joints.

The rotation point under the U-shaped profile facilitated an elevation plane of 0.8 to1.5rad. With a fixed rotation point the prototype was able to be moved approximately 0.2rad out of the elevation plane without noticeable compromise on the support.

The maximum distance from the prototype to the arm was 59mm. Despite that it is smaller than the WREX (65mm) it is larger than the requirement of 20mm to the body. However, the width of one beam in combination with 2 wires is 7.5mm, so if the beam is situated close to the arm it has the potential to fit within 20mm from the body. One option to situate it closer to the arm is to place B2 at the sides of the cup, instead of under the cup.

The width of the elastic and structural elements of WREX in the vicinity of the upper arm is measured to be 32mm. The width of these elements in the prototype with beams (7.5mm) is more than 4 times smaller than in the WREX. Together with the fact that the prototype follows human anatomy, it makes it a promising design for a wearable arm support.

IX. Conclusion

The goal of this research was to propose a concept for an upper arm support that fits within 20mm around the body. An arm support was presented that uses beams to balance the arm. With this method no other structural elements than wires are needed to support the arm. In this way the device can be made smaller than the conventional designs which consist of springs and structural rods. Simulations showed that two beams made of CFRP and with dimensions 0.22x0.0041x0.0027m can store enough energy to support the arm during eating. These beams can balance the upper arm, by placement of the rotation point of the beams vertically under the rotation point of the wires.

A prototype was made for evaluation of the balancing capabilities of the beams. The arm was balanced more than 87% until 1.1rad, which corresponded to the simulations.

A second prototype was made to test the concept in relation to the human arm. It resulted in a prototype with a width of 7.5mm at both sides of the arm for both the elastic element (beam) and structural elements (2 wires). This is more than four times smaller than the current orthoses. It can fit within the 20mm limit, if the beam and wires are situated close to the arm.

In order to make the device feel comfortable, the device was designed so that no shear forces were exerted on the skin. This was verified by the second prototype, which did not show displacements between the skin of the arm and the device during elevation.

From the simulations, prototypes and measurements it can be concluded that bending beams have the potential to make an orthosis that is closer to the upper arm than current orthoses.

Acknowledgment

This research is supported by the Flextension project (STW11832) of the Dutch Technology Foundation STW, which is part of the Netherlands Organisation for Scientific Research (NWO), and which is partly funded by the Ministry of Economic Affairs.

References

[1] A. E. H. Emery, “Population frequencies of inherited neuromuscular diseases - a world survey,” *Neuromuscular Disorders*, vol. I, no. I, pp. 19–29, 1991.

[2] T. Rahman, W. Sample, R. Seliktar, M. Alexander, and M. Scavina, “A body-powered functional upper limb orthosis.” *Journal of rehabilitation research and development*, vol. 37, no. 6, pp. 675–80, 2000.

[3] A. G. Dunning and J. L. Herder, "A review of assistive devices for arm balancing," *International Conference on Rehabilitation Robotics*, pp. 1–6, Jun. 2013.

[4] T. Rahman, S. Stroud, R. Ramanathan, and M. Alexander, "Task priorities and design for an arm orthosis," *Elsevier Technology and Disability*, no. 5, pp. 197–203, 1996.

[5] L. F. Cardoso, S. Tomazio, and J. L. Herder, "Conceptual design of a passive arm orthosis," *ASME, International Design Engineering Technical Conferences*, pp. 747–756, 2002.

[6] M. M. H. P. Janssen, A. Bergsma, A. C. H. Geurts, and I. J. M. de Groot, "Patterns of decline in upper limb function of boys and men with DMD: an international survey." *Journal of neurology*, vol. 261, no. 7, pp. 1269–1288, Jul. 2014.

[7] J. Herder, "Development of a Statically Balanced Arm Support: ARMON," *International Conference on Rehabilitation Robotics*, pp. 281–286, 2005.

[8] C. J. van Andel, N. Wolterbeek, C. a. M. Doorenbosch, D. H. E. J. Veeger, and J. Harlaar, "Complete 3D kinematics of upper extremity functional tasks." *Gait & posture*, vol. 27, no. 1, pp. 120–7, Jan. 2008.

[9] D. A. Winter, *Biomechanics and motor conrol of human movement*, 4th ed. John Wiley & Sons, inc., 2009.

[10] G. Radaelli and J. L. Herder, "Isogeometric Shape Optimization for Compliant Mechanisms with Prescribed Load Paths," *ASME International Design Engineering Technical Conferences*, pp. 1–11, 2014.

[11] J. Austin Cottrell, T. J. R. Hughes, and J. Bazilevs, *Isogeometric Analysis: Toward Integration of CAD and FEA*. John Wiley & Sons, Inc., 2009.

[12] L. Piegl and W. Tiller, *The NURBS book*, 2nd ed. Springer, 1997.

[13] A. P. Nagy, M. M. Abdalla, and Z. Gürdal, "Isogeometric sizing and shape optimisation of beam structures," *Computer Methods in Applied Mechanics and Engineering*, vol. 199, no. 17-20, pp. 1216–1230, Mar. 2010.

[14] *Hexcel, www.hexcel.com/Resources/Cont-Carbon-Fiber-Data-Sheets*.

Appendix A

Requirements

A-1 Requirements

The requirements of the device:

- Unobtrusive: The orthosis is considered unobtrusive if it is closer than 2cm to the body. In that way it will fit underneath clothing that is one size bigger than the person usually wears. Under the armpit up to 5 cm of space is available.
- Comfortable: A large variety exist between values of allowable pressure on the skin without tissue degeneration. This reaches for longterm pressure from 4kPa [1](tissue covering bony prominences) to 250kPa [2](finger top). For the situation of short term pressure on the upper arm, no data is available. The lowest allowable pressure(4kPa) results in an area of support necessary:

  $$\frac{3.84 * 9.81 * sin(1.1)}{4000} = 0.0084m2$$

  This results in a maximum of 84cm2 necessary to support the arm. Because it is not continuous support(and not tissue covering bony prominences), it is expected that an area which is a factor 1-100 smaller could be large enough for having a comfortable support.

  Even about the shear force no guideline could be substracted from literature, besides that shear force on the skin should be kept very low. Therefore user tests should reveal if the forces of the device on the arm feel comfortable or not. The functioning of the sweat gland should not not be obstructed, so no pressure on the axilla is aloud.
- Support eating movement: The upper arm is elevated during the eating motion from 0.3 to 1.1rad [3]. This is the range for which the device should assist the upper arm for at least 90%. A person with unaffected muscles uses a maximum of 9.5Nm to elevate

the arm during eating movement [4]. This means that the device should work properly with an activation of approximately 0.95Nm around the shoulder.

- Velocity: The device should support the patient to be able to eat with a normal eating velocity and acceleration. The peak velocity during eating is 430 mm/s [5]. Assuming an upper arm of 34 cm, this results in a required angular velocity of 72 degrees/second.

Assumption:

- It is assumed that the device can be rigidly connected to the trunk by a corset. Corsets are worn by people with Duchenne for stabilizing the trunk. This assumption excludes the development of a structure for transporting the forces of the device to the trunk from the project.

A-2 Pictograms of requirements and assumptions

The following figure shows the pictograms that were designed for explanation of the requirements and assumptions. The pictograms about rotation and elevation are faded because the focus for the orthosis will be on assisting the elevation.

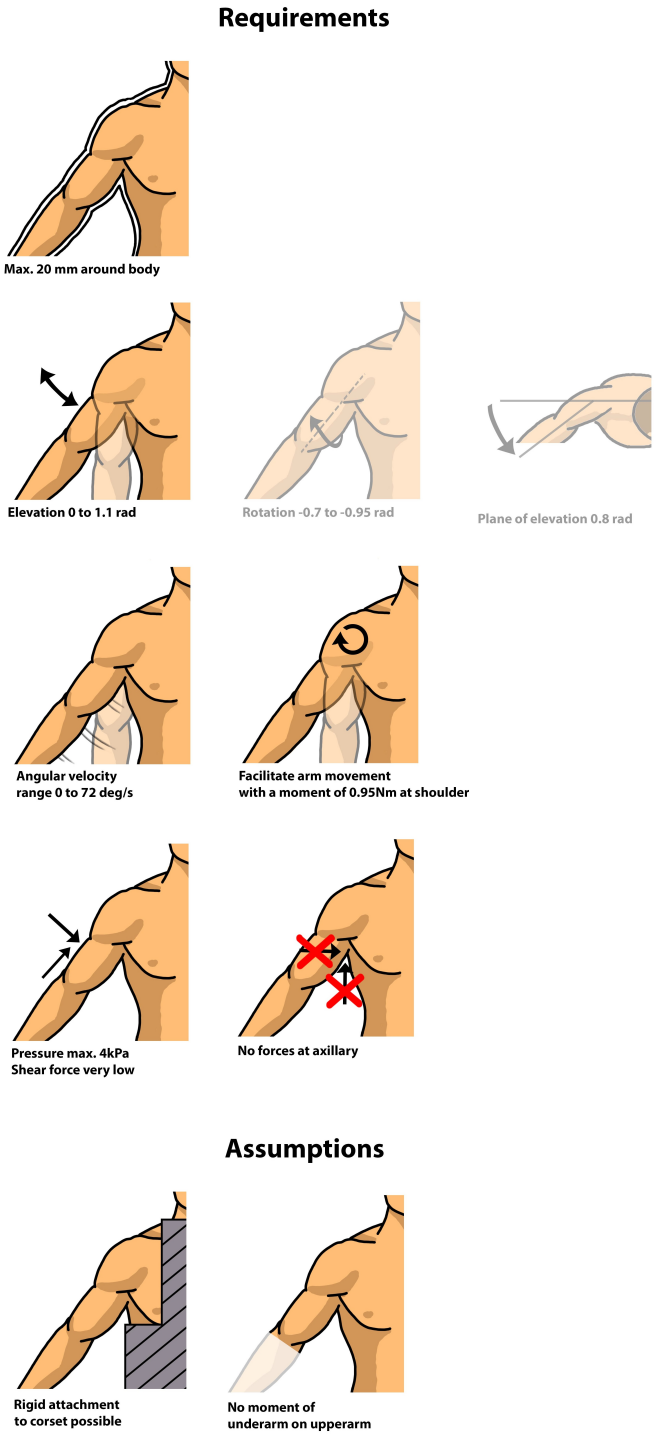

Appendix B

Analysis

B-1 Anthropomorphic data

No data of length and weight of Duchenne patients was available. Therefore the calculations are done with data of average dutch men. An average dutch men(age 18-30) has a length of 1.84m and a mass of 77kg according to Dined [6].

Winter [7] calculated the ratio between the length and weight of the body to parts of the body as follows:
Length upper arm=0.186*length body
Weight upper arm=0.028*weight body
Weight forearm=0.016*weight body
Weight hand=0.006*weight body
Distance center of mass from glenohumeral joint=0.436*length upperarm

This results in:
Length upper arm=0.184*1.84=0.34m
Weight upper arm=0.028*77=2.16kg
Weight forearm+hand=(0.016+0.006)*77=1.69kg
Total weight=1.69+2.16=3.85kg
Distance center of mass from glenohumeral joint=0.436*0.34=0.15m
Distance center of mass total arm: CoMTot=(mu*larm+CoM*m)/(mTot)=0.23m

B-2 Representation arm

The following figure = shows the simplification of the arm.

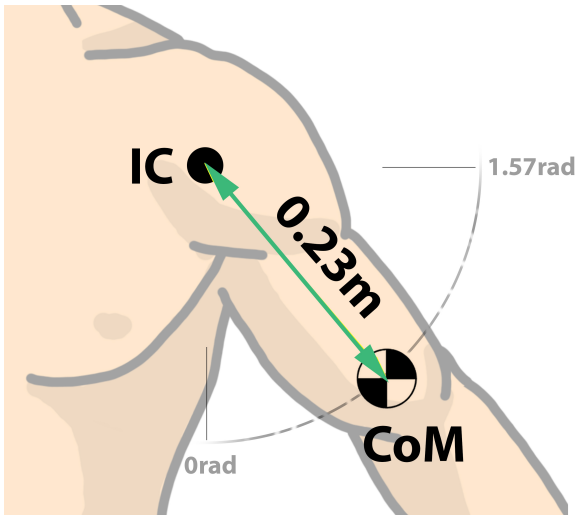

The maximum acceleration(α) during an eating movement is 0.6rad/s^2. The mass moment of inertia of the arm is:

$$I = m * r^2 = 0.20Nm^2$$

The maximum moment(M) working on the shoulder due to inertia is:

$$M = I * \alpha = 0.12Nm]$$

This is a factor 65 smaller than the required moment for balancing the arm at 1.1rad and therefore not taken into account.

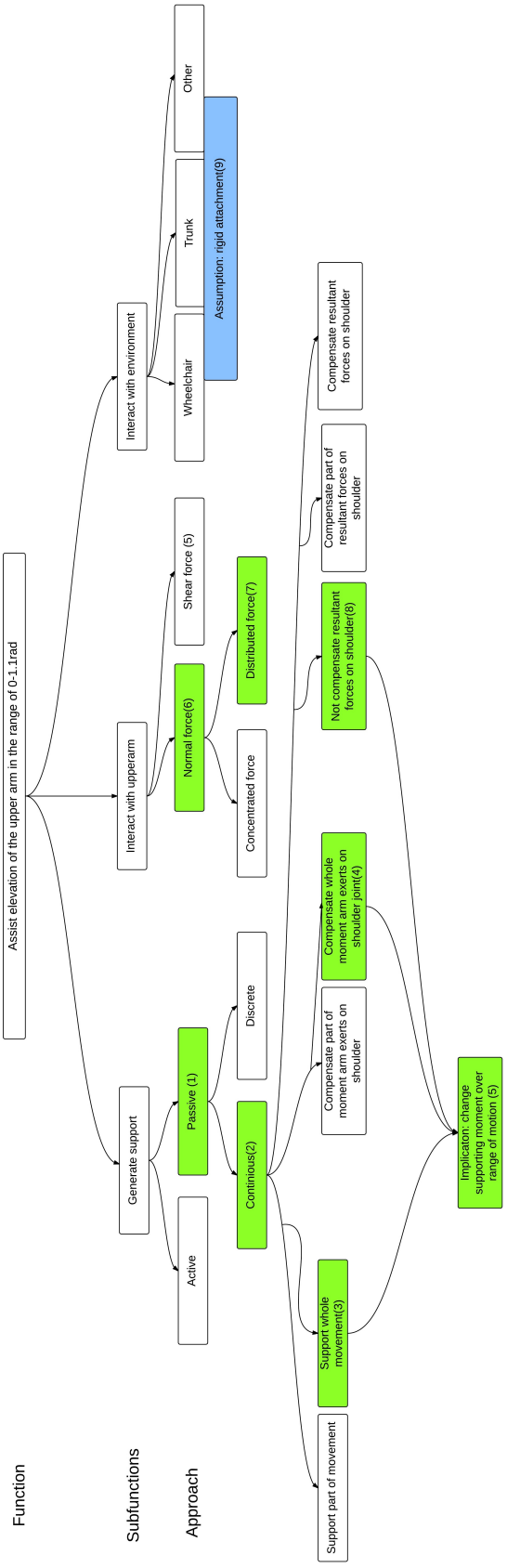
Function
Subfunctions
Approach
Assist elevation of the upper arm in the range of 0-1.1rad
Interact with environment
Interact with upperarm
Generate support
Wheelchair
Trunk
Other
Assumption: rigid attachment(9)
Normal force(6)
Shear force (5)
Concentrated force
Distributed force(7)
Passive (1)
Active
Discrete
Continious(2)
Support part of movement
Support whole movement(3)
Compensate part of moment arm exerts on shoulder
Compensate whole moment arm exerts on shoulder joint(4)
Not compensate resultant forces on shoulder(8)
Compensate part of resultant forces on shoulder
Compensate resultant forces on shoulder
Implication: change supporting moment over range of motion (5)

B-3 Function specification and approach

The figure shows the function specification and approach. The green blocks present the approach that was chosen.
(1) No need for actuators - smaller
(2) More natural feeling
(3) Freedom to stop within a movement
(4) Useful for patients with very low muscle force
(5) Statically balanced mechanism
(6) Considered as more comfortable than shear forces
(7) Considered as more comfortable than concentrated force
(8) These forces can only be compensated on the upper arm if shear forces are involved. Shear forces should be low so therefore no compensation for forces on the shoulder joint.
(9) The development of a structure for transporting the forces of the device to the environment is behind the scope of this project.

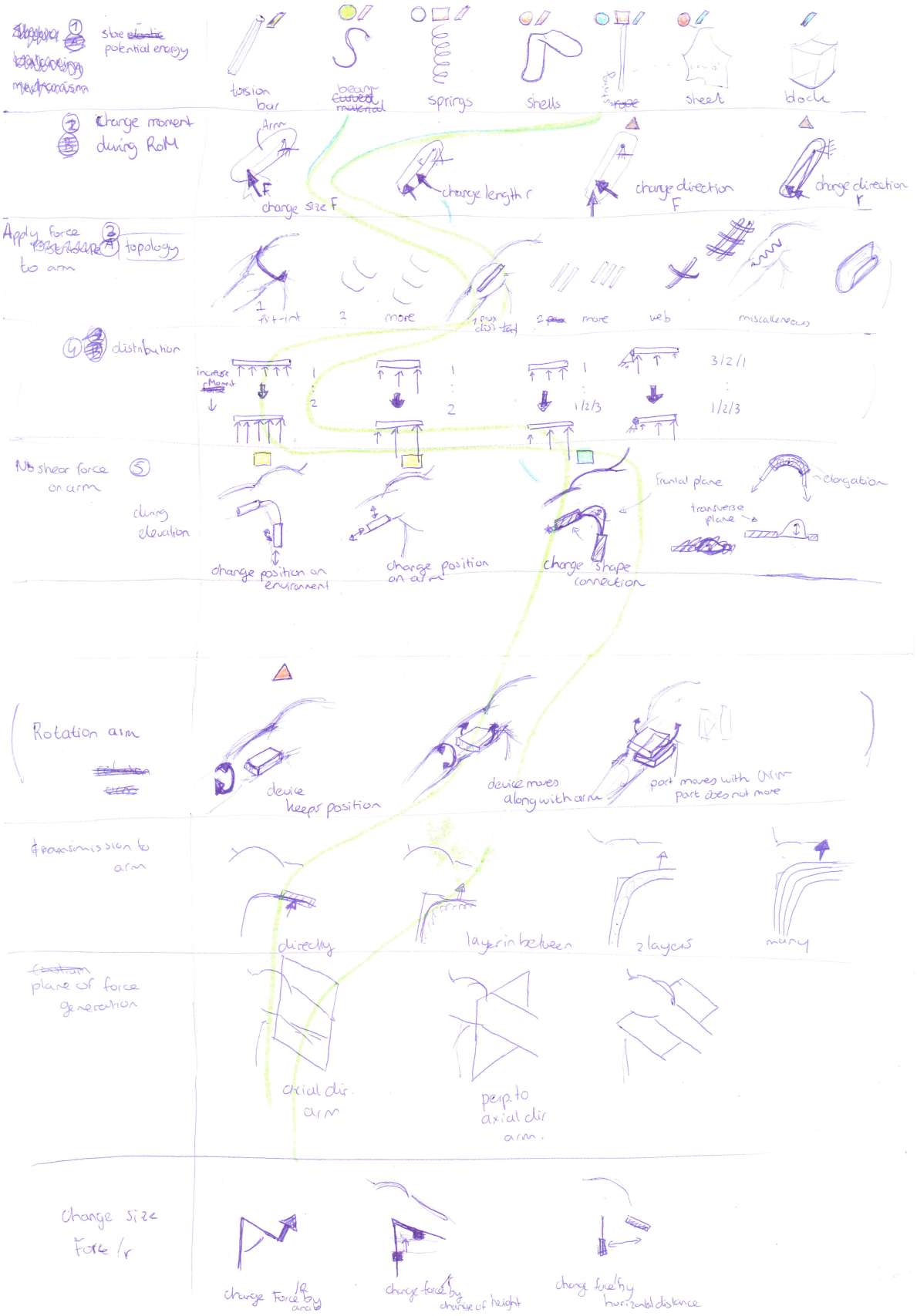
store potential energy
torsion bar
beam
springs
shells
sheet
block
charge moment during RoM
Arm
F
charge size F
charge length r
charge direction F
charge direction r
Apply force to arm
topology
1 fit+int
2
more
1 pair dist tied
2 pairs
more
web
miscellaneous
distribution
increase Moment
1 : 2
1 : 2
1 : 1/2/3
3/2/1 : 1/2/3
No shear force on arm
during elevation
charge position on environment
charge position on arm
charge shape connection
frontal plane
elongation
transverse plane
Rotation arm
device keeps position
device moves along with arm
part moves with arm part does not move
transmission to arm
directly
layer in between
2 layers
many
plane of force generation
axial dir arm
perp. to axial dir arm.
Change size Force / r
charge Force/R by angle
charge force by change of height
charge force by horizontal distance

Appendix C

Conceptual design

C-1 Morphological chart

A morphological chart was made to get inspiration for concepts and to reveal a large range of options. The functions in the first column are subtracted from the function specification and requirements.

Specification of the rows:

1. The ways to store potential energy. Rectangle represent options that potentially fits within 2cm layer. The stripe indicates a high(green) or lower(red) energy storage versus volume ratio. A circle is added if theory is available about statically balancing with this mechanism.
2. Change moment during range of movement. Change direction + change r ; not suitable because results in shear forces on upper arm(triangle).
3. Topology of applied force.
4. Distribution of force on arm.
5. No shear force on arm during elevation. Change position on arm/environment need at least two layers, while changing the shape of the connection only needs one.
6. Options for providing arm rotation.
7. Transmission to arm.
8. Plane of force generation.
9. Change size of force by geometric relation.

#1 Block

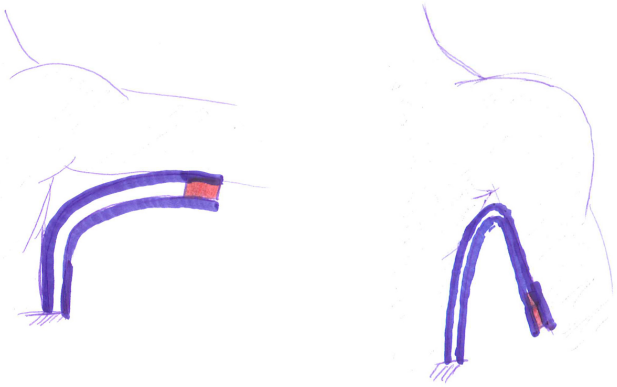

#2 Sandwich

#3 Double beam

#4 Springs

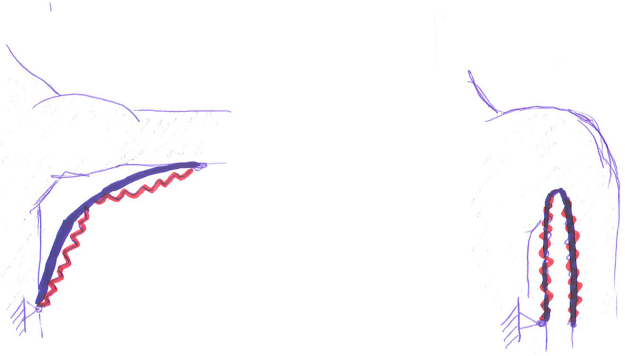

C-2 Concepts

The options in the morphological chart were combined to several concepts. The figure shows four concepts which uses different methods for storing energy. The elastic energy in the device should be largest when the arm is pointing down and during elevation the energy should be released.
The first concept stores the energy in a block, that is compressed by change of the shape of two surrounding beams. The second concept stores energy in small beams that change shape during elevation. The third concept releases energy by the change of two beams. The last concept stores energy in helical springs or rubber bands. During elevation the distance of the attachment points becomes smaller and therefore energy is released.

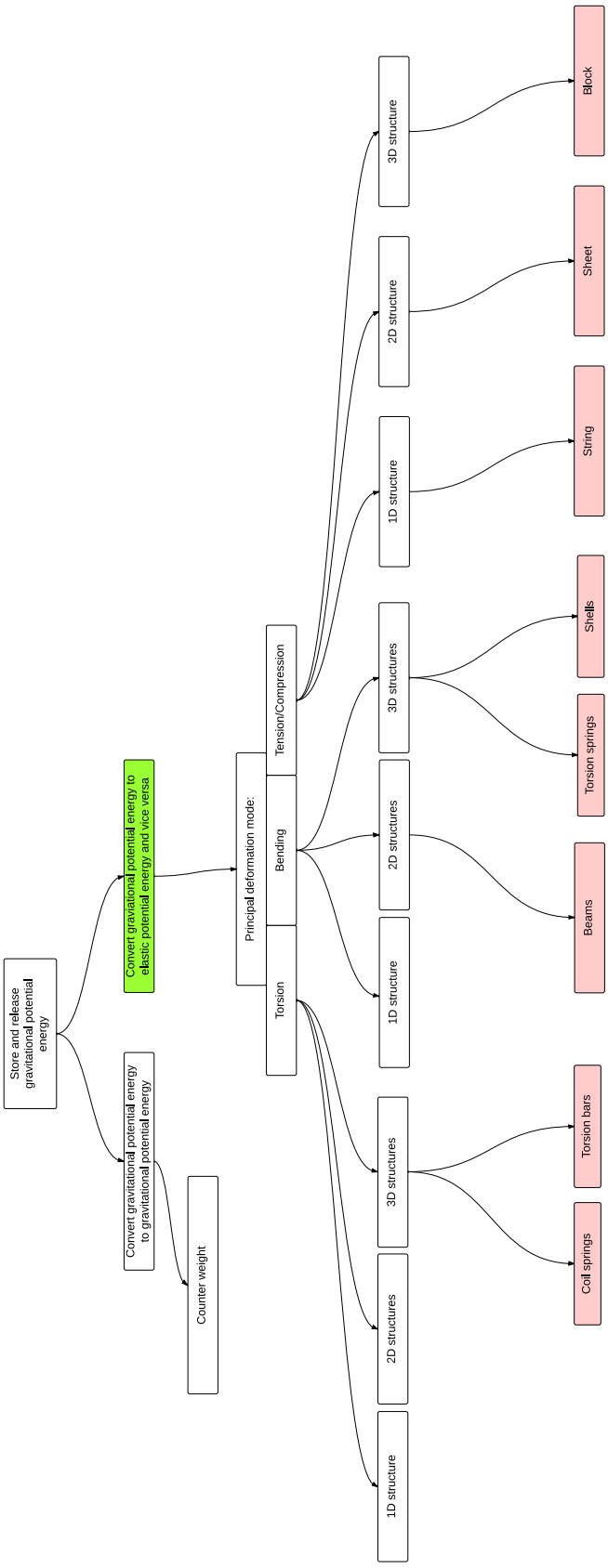
Store and release gravitational potential energy
Convert gravitational potential energy to elastic potential energy and vice versa
Convert gravitational potential energy to gravitational potential energy
Counter weight
Principal deformation mode:
Torsion
Bending
Tension/Compression
1D structure
2D structures
3D structures
1D structure
2D structures
3D structures
1D structure
2D structure
3D structure
Coil springs
Torsion bars
Beams
Torsion springs
Shells
String
Sheet
Block

C-3 Principals storing elastic energy

The principle of storing potential energy was of major importance for the feasibility of the concepts. The pink blocks in the figure show the options for storing elastic energy. The options are categorised by deformation mode and dimension of the elements.

Energy storage principal:	Coils springs	Torsion bars	Beams	Torsion springs	Shells	Strings	Sheet	Block
Requirements:								
Invisible								
Store energy efficiency(1)								
Integration structural+elastic elements(2)								
Support								
Balance 90%(3)								
Friction between elements (green is low friction)(4)								
Eating movement(5)								
Range of motion								
Velocity								
Acceleration								
Comfortable(6)								
Low shear force								
No forces at axilla								

C-4 Comparison storing energy methods

The table shows the comparison between the eight options for storing elastic energy. Explanation:
(1) In tension and compression the most energy can be stored(green) because all the material can strain to its maximum. Bending and torsion are less efficient deformation modes because only the outer material stores maximum energy(yellow). (evt. ref)
(2) A supporting force under de arm is required to assist the arm. With coil springs, torsion springs, strings or sheets alone this is not possible because it only can exert pulling forces. With these principals always a linkage is required to convert the tension to a supporting force(red). Torsion bars and blocks can exert a pushing force, but with these principals it is likely that the energy is stored in a part of the design, whereas another part functions as structure(yellow). Beams and shells are marked green because the elastic elements can be the structure of the design.
(3) It is proven that with coil springs, beams and strings(rubbers) it is possible to balance a mass around a rotation point between 0 and 1.6 rad(green). For torsion bars, torsion springs, shells, sheets and blocks it remains unsure if it has the ability to balance a mass(yellow).
(4) With beams and shells the structural and elastic elements can be integrated, therefore having the potential to contain less sliding parts, and as a result less friction(green) than the other principals(yellow).
(5)/(6) If the RoM, velocity and acceleration of the eating movement is provided by the device, depends mainly on the design instead of the energy storage principal. The same holds for the low shear forces and no forces at axilla. Therefore these blocks are marked neutral(grey).

C-5 Three options with beams

The following figure shows three options that possibly can support an arm with the use of beams.

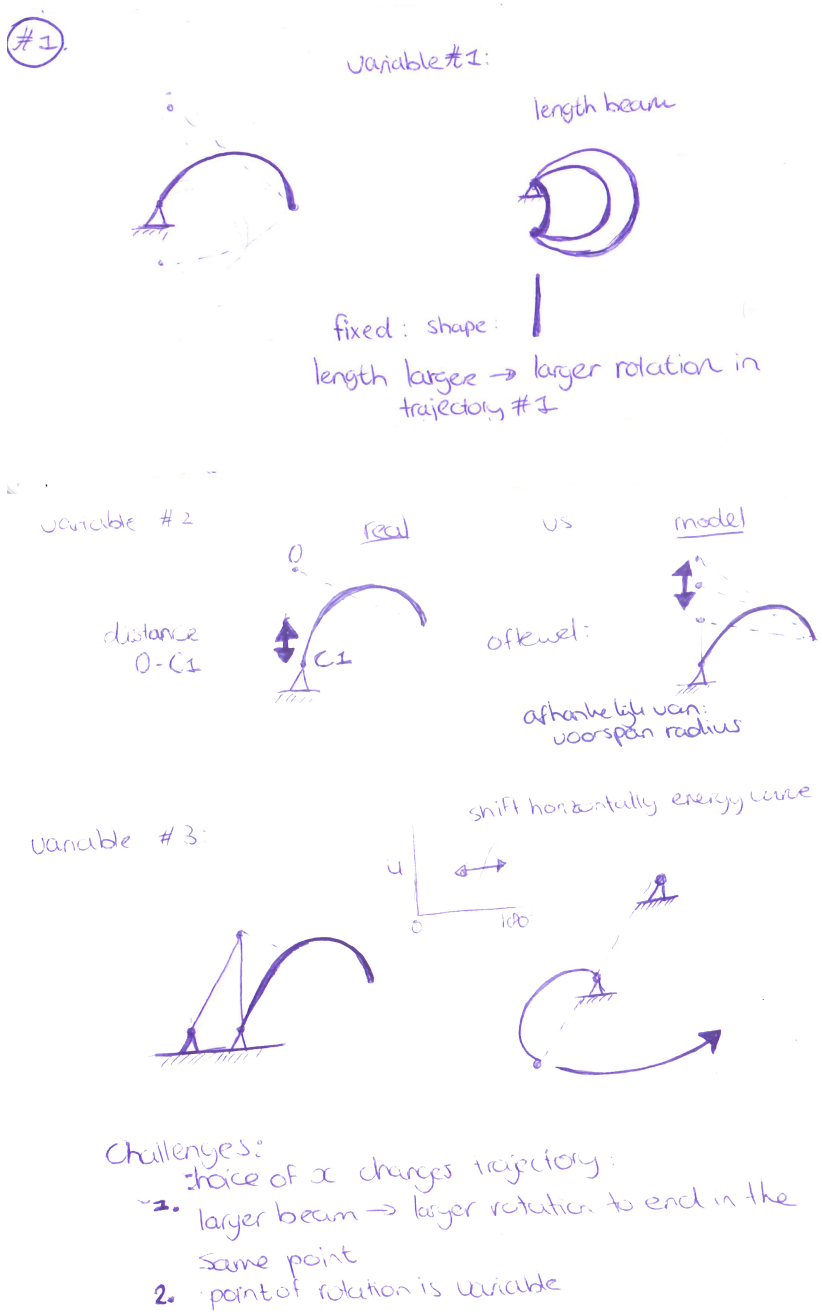

Figure C-1

Disadvantage: thick beams required for moment

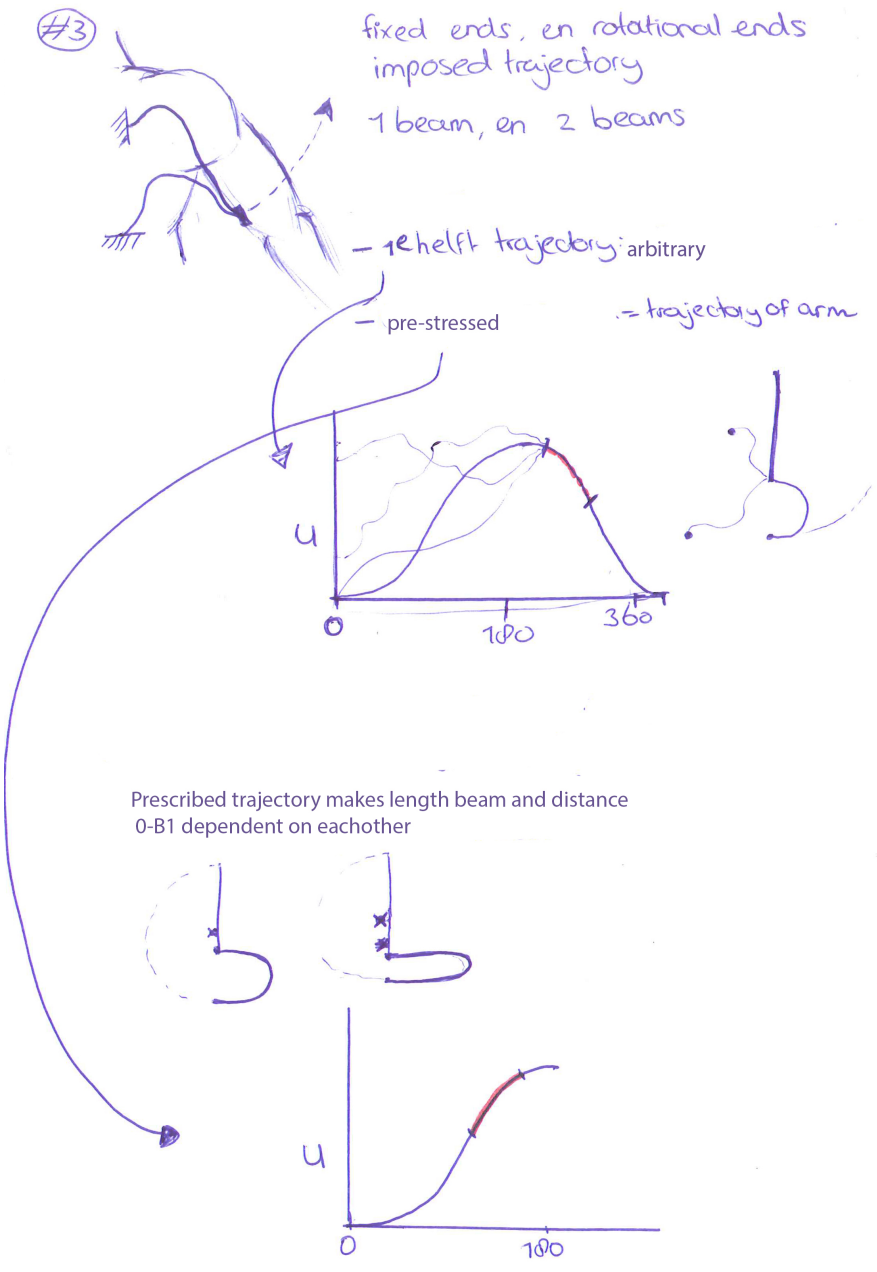

Prescribed trajectory makes length beam and distance 0-B1 dependent on eachother

Figure C-2

Appendix D

Dimensional design

D-1 Influence distance IC-B1

Table D-1 shows the properties of the beams for 3 different options of the distance IC-B1.

Unnormalised									
IC-B1(m)	IC-B2(m)	max elev.(rad)	Length beam(m)	Deviation(Nm)	Max dev.(Nm)	Max Fic(N)	Thickness	Width(m)	Volume(m^3)
0.0125	0.23	1.1	0.225	1.64	0.13	351	0.0043	0.0023	2.23E-06
0.025	0.23	1.1	0.220	2.31	0.20	173	0.0027	0.0040	2.38E-06
0.05	0.23	1.1	0.212	4.98	0.43	86	0.0018	0.0068	2.59E-06
Normalised									
1.00	1.00	1.00	1.00	1.00	1.00	1.00	1.00	1.00	1.00
2.00	1.00	1.00	0.98	1.41	1.50	0.49	0.64	1.74	1.12
4.00	1.00	1.00	0.94	3.04	3.30	0.25	0.41	2.96	1.23

Table D-1

D-2 Comparison spring steel/fibre glass/CFRP

Table D-2 shows the comparison of springsteel (Sandvik 11R51) [8], Fibre glass [9] and CFRP (Hexel AS7, 50% fibre) [10]. The numbers presented are not representative for all the spring steel/fibre glass/CFRP because a large variety of types exist, with deviating material properties.

An orthosis close to the body require beams that can store a large amount of energy while having a limited width. The table shows that fibre glass has the largest strain limit, but the lowest stiffness. An orthosis made with spring steel results in beams with a total width of 24.2mm. This could be for example one beam (width 12.1mm) at both sides of the arm, or 2 stacked beams (width 6.1mm) at both sides of the arm.
However, with CFRP beams only one beam of 4.2mm is required at both sides of the arm to

	Spring steel	Fibre glass	CFRP
Tensile strength (Pa)	2.30e9	1.03e9	4.90e9
Youngs modulus (Pa)	1.90e11	4.48e10	2.42e11
Strain limit* (-)	6.05e-3	1.15e-2	1.01e-2
Thickness** (m)	1.64e-3	3.11e-3	2.73e-3
Width*** (m)	2.42e-2	1.50e-2	8.19e-3

Table D-2: Comparison of springsteel, fibre glass and CFRP. Beams of CFRP have the smallest width for storing the same amount of energy.*The strain limit was set to 50% of the strain at tensile strength. **The allowable thickness, within the strain limit. ***The width required to store enough energy for elevating the arm.

store enough energy for lifting the arm. Due to the high tensile strength and elastic modulus of carbon fibre it can store the most energy compared to its width. Therefore this material was chosen for the beams of the final design.

Appendix E

Prototype #1

E-1 Beams

E-1-1 Material

The material used for the beams has a thickness tolerance of ś0,013mm, tensile strength of 1500-1700 N/mm and elastic modulus of 180GPa. Other specifications are shown in Fig. E-1 [11].

Material 1.4301		
stainless and acid-resisting steel	Chemical Analysis:	
X 5 Cr Ni 18 9	C = max. 0,07%	Cr = 17 - 20,0%
US-Norm AISI 304	Si = max 1,00%	Ni = 8,5 - 10,0%
AFNOR Z 6 CN 18-09	Mn = max. 2,00%	
cold-rolled, spring-grade hardness	P = max. 0,045%	
clean surface	S = max. 0,03%	

Figure E-1: Specifications of the material used for the beams.

E-1-2 Dimensions

The length required for a straight beam at 1.75rad is 0.206m. The beams with thickness 0.7mm have a width of 7.5mm, the beams with thickness 0.8mm a width of 5.0mm.

E-2 Arm

The mass of the arm is 0.54kg. The dimensions of the "arm" in centimeter:

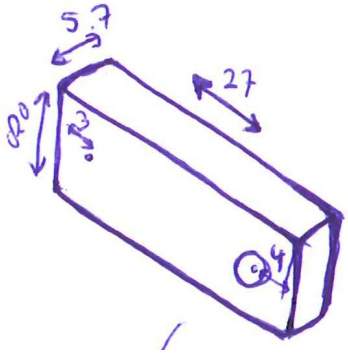

E-3 Photos of prototype #1

Figure E-2: Front view of prototype #1.

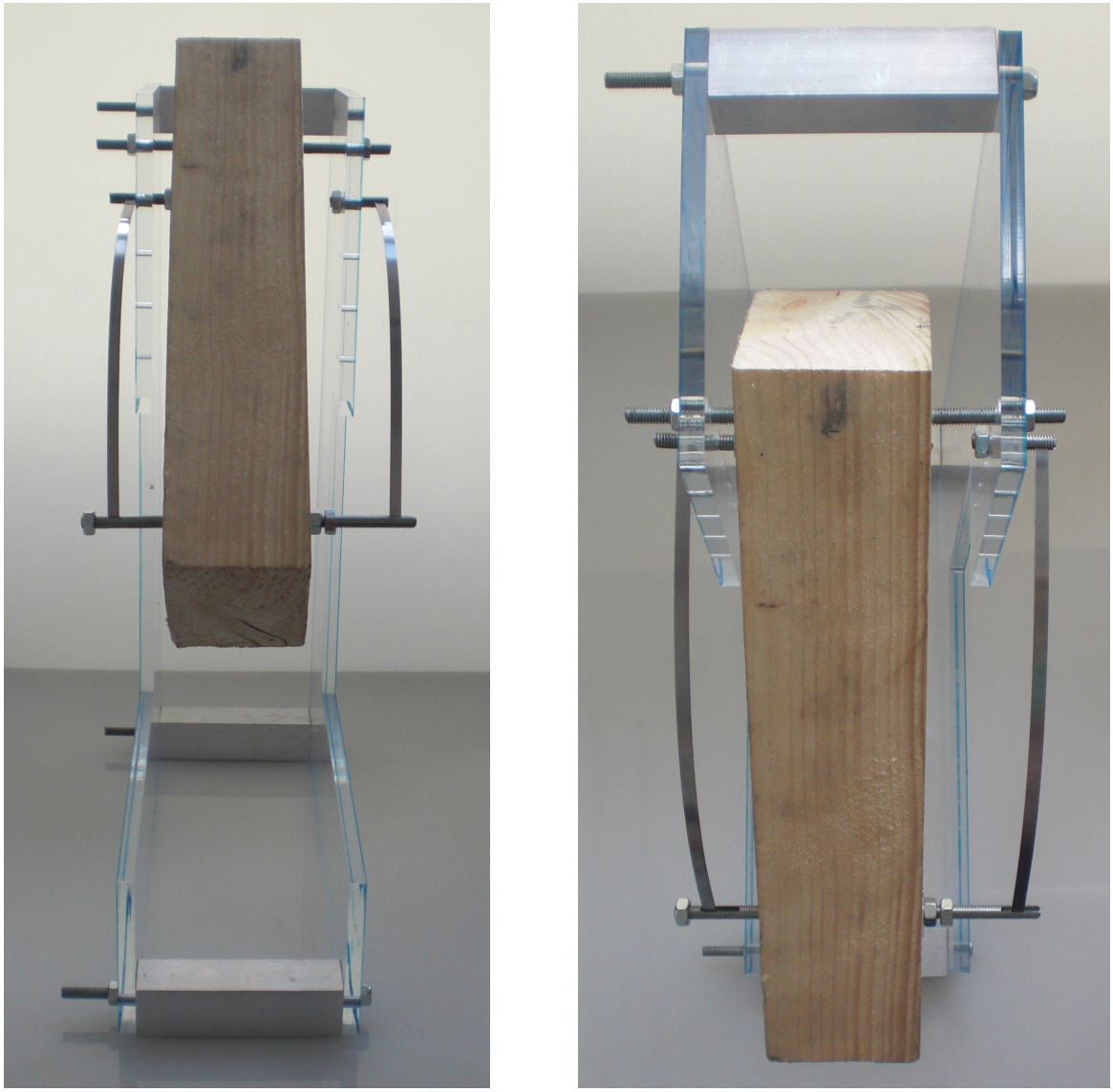

(a) Side view **(b)** Top view

Figure E-3: Prototype #1

Appendix F

Measuring and data processing prototype #1

F-1 Setup

The modules of the measurement setup are:

- Breadboard (Thorlabs PBG51522, dim. 600x450x25)
- Linear motor stage (Physik Instrumente M-505.4DG, resolution: 0.05ţm, travel range: 100mm)
- Force sensor (Futek LSB200, resolution 2mV/V, range: 0-44.5N)
- Data amplifier (ICP DAS 3016)
- Data acquisition module (National Instruments USB6008)

The software used to record and process the data are:

- Labview 12 National Instruments.
- Matlab R2014a

The calibration factor for the force sensor was set to 3.77 N/V. This was checked with a spring balance. With the 'zero' screw on the data amplifier the force sensor was set to zero, when no load was applied.

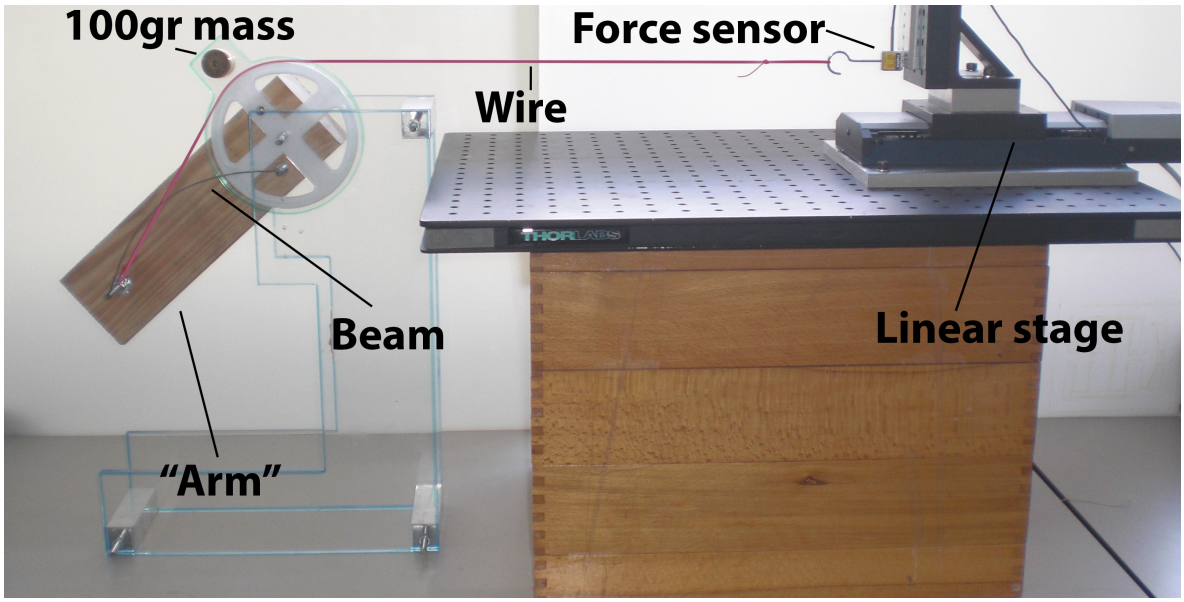

Figure F-1: The front view of the setup for evaluation of the moment that is balanced by prototype #1.

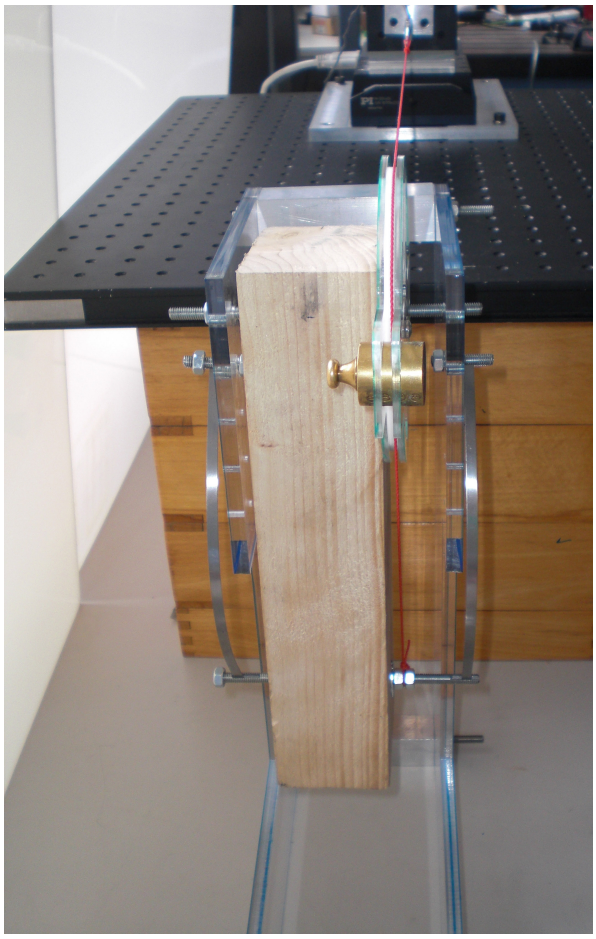

Figure F-2: The side view of prototype #1 with measurement set-up.

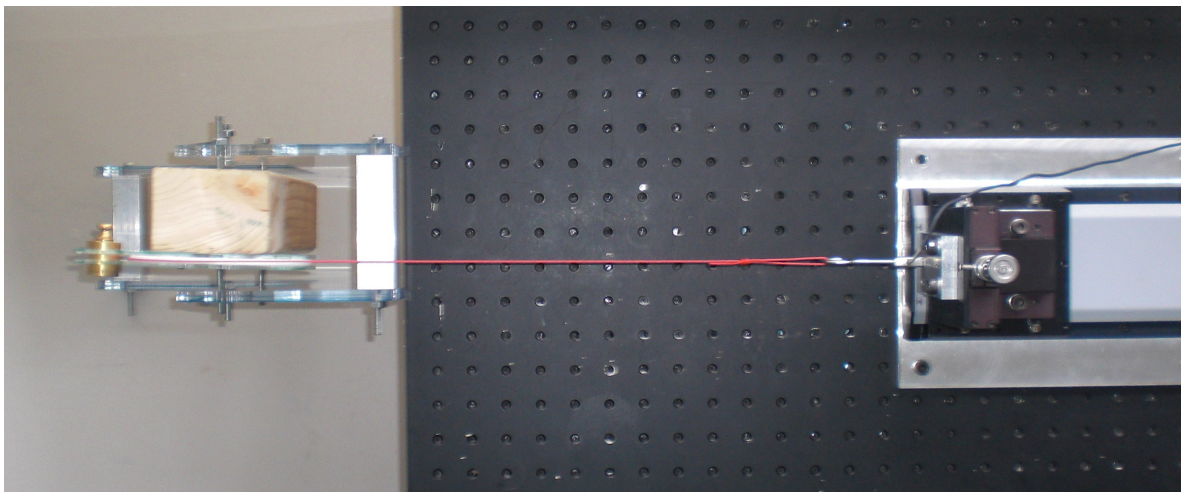

Figure F-3: The top view of prototype #1 with measurement set-up.

F-2 Measurement protocol

The protocol of measurement:

1. Move the stage to the beginning of the slider.
2. Connect the wire to the "arm" and to the force sensor. The wire should be slightly tensed when the "arm" is pointing down.
3. Align the pulley of the prototype with the force sensor. Adjust the height of the force sensor to the height of the wire on the pulley.
4. Start Labview, select file: MeasurementSetup.vi
5. Fill in the file name of the measurement
6. Fill in -107000 µm as the distance to travel
7. Press RUN.
8. When the linear motor stage is at its end position, fill in -107000 µm
9. Press RUN to return to start position.

Table F-1 presents the experiments that were done. These parameters varied:

- Number of beams
- Thickness of beams
- Position (for one beam)
- With or without a 100gr mass attached to the pulley.

Experiment	Nr. of beams (position)	Thickness of beam(s)	Weight:No(0)/Yes(1)
1	0	-	0
2	0	-	1
3	1(front)	0.8mm	1
4	1(back)	0.8mm	1
5	2	0.8mm	0
6	2	0.8mm	1
7	2	0.8mm	1
8	2	0.7mm	1

Table F-1: The eight experiments that were executed.

F-3 Data processing protocol

The protocol of data processing:

1. Delete last part of data (if measurement was not stopped at end of displacement).

2. Convert data from linear displacement of the stage to rotation of the "arm" in radians.
3. Smooth force data with a moving average filter(span 100).
4. Convert force data to data of the force only in the direction perpendicular to "arm".
5. Substract the effect of the 100gr mass (if applicable)
6. Linearly interpolate data at 0.01rad instances (for averaging multiple sets of data that are sampled at different points)

Appendix G

Results of measurements prototype #1

Fig. G-1 shows both the raw data and the smoothened+interpolated data of experiment 6. From this figure it can be concluded that the smoothening and interpolation does not influence the trend of the data.

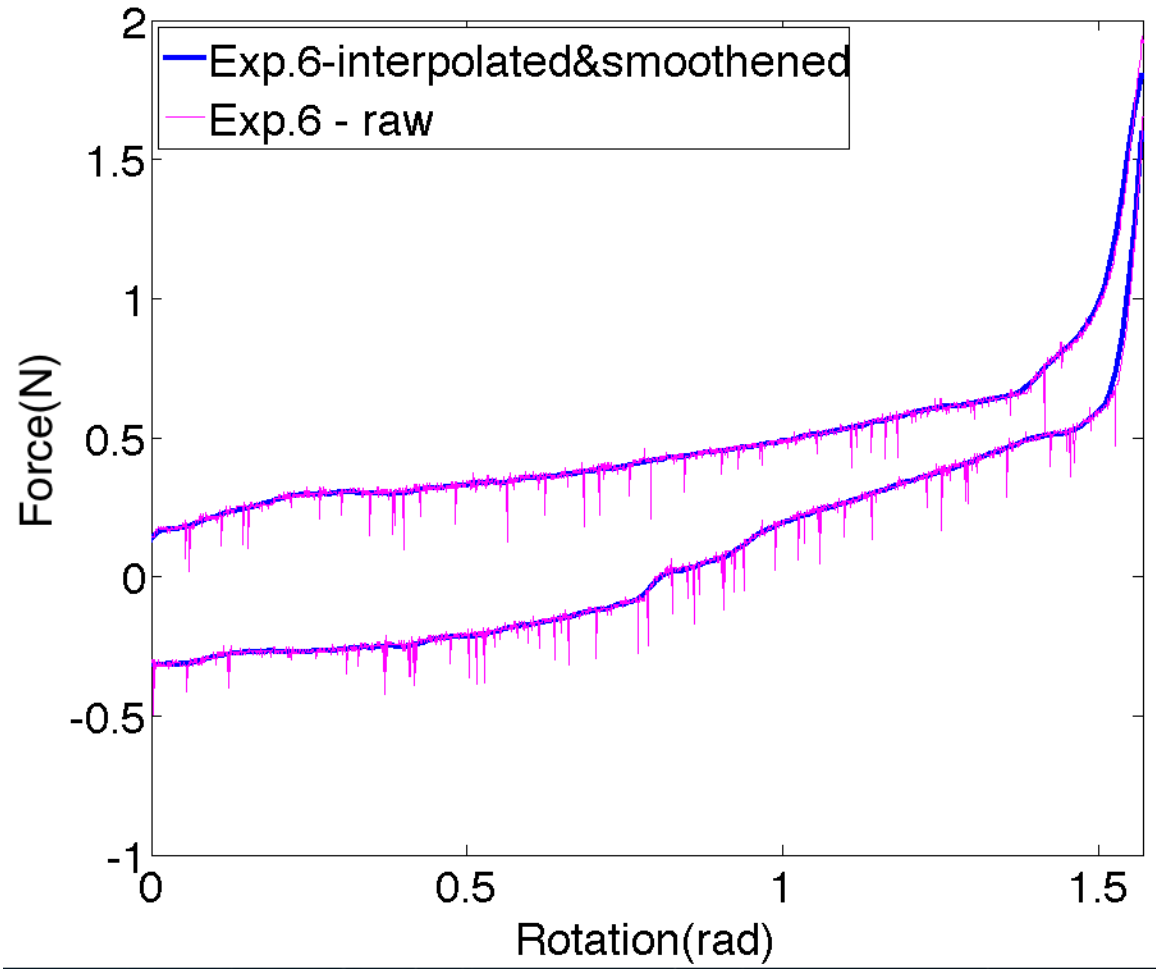

Figure G-1: Force-rotation characteristic of experiment 6 for the raw data (pink) and processed data (blue).

The force to lift the "arm" is:

$$m * g * cos(\alpha)$$

m is the mass of the arm, g the gravitational force and α the rotation of the arm. Fig. G-2 shows the average of the measured data (Exp. 1), and the expected data. The average of the measured force of the movement up and down corresponds with the expected data.

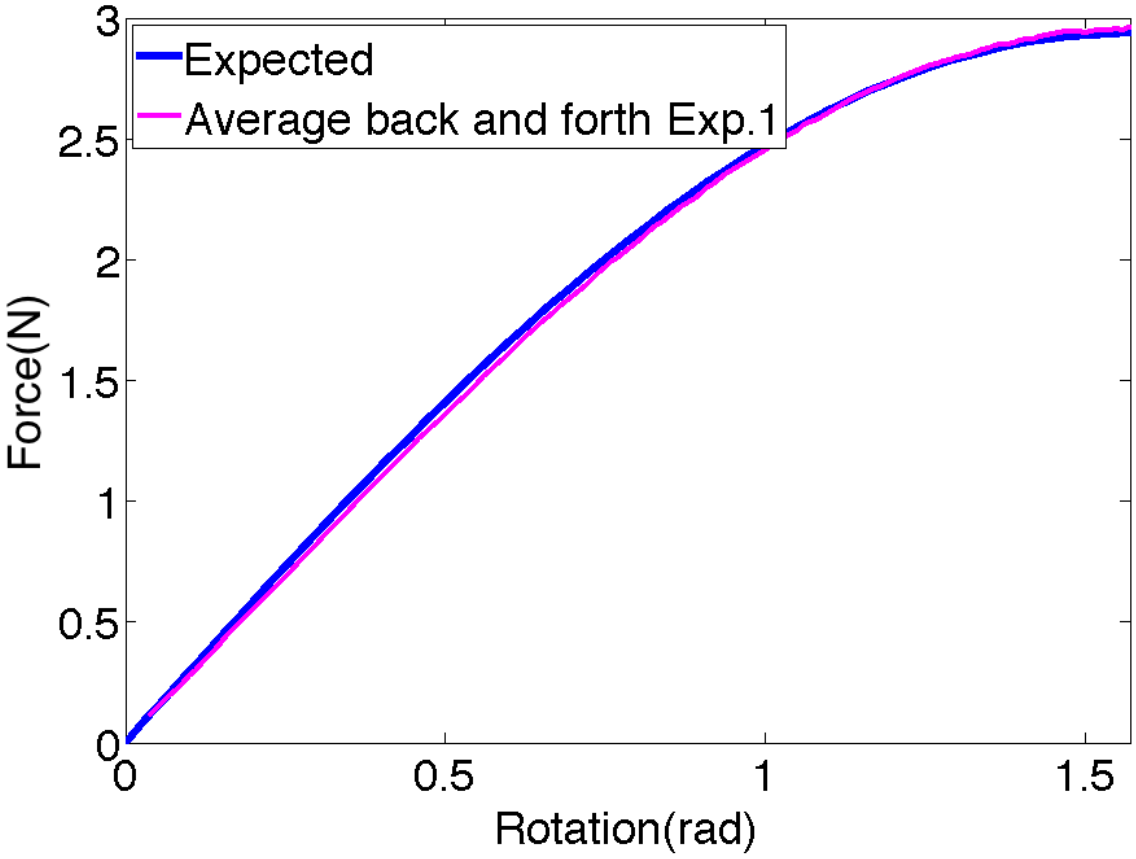

Figure G-2: Force-rotation characteristic of the unbalanced arm with calculations(blue) and experiments(pink).

Fig. G-3 shows the data of the experiments with(Exp. 1) and without(Exp. 2) an extra 100gr mass. The effect of the mass was subtracted from the force data of experiment 1. It can be concluded that the extra mass slightly increased the friction for rotations smaller than 0.75rad.

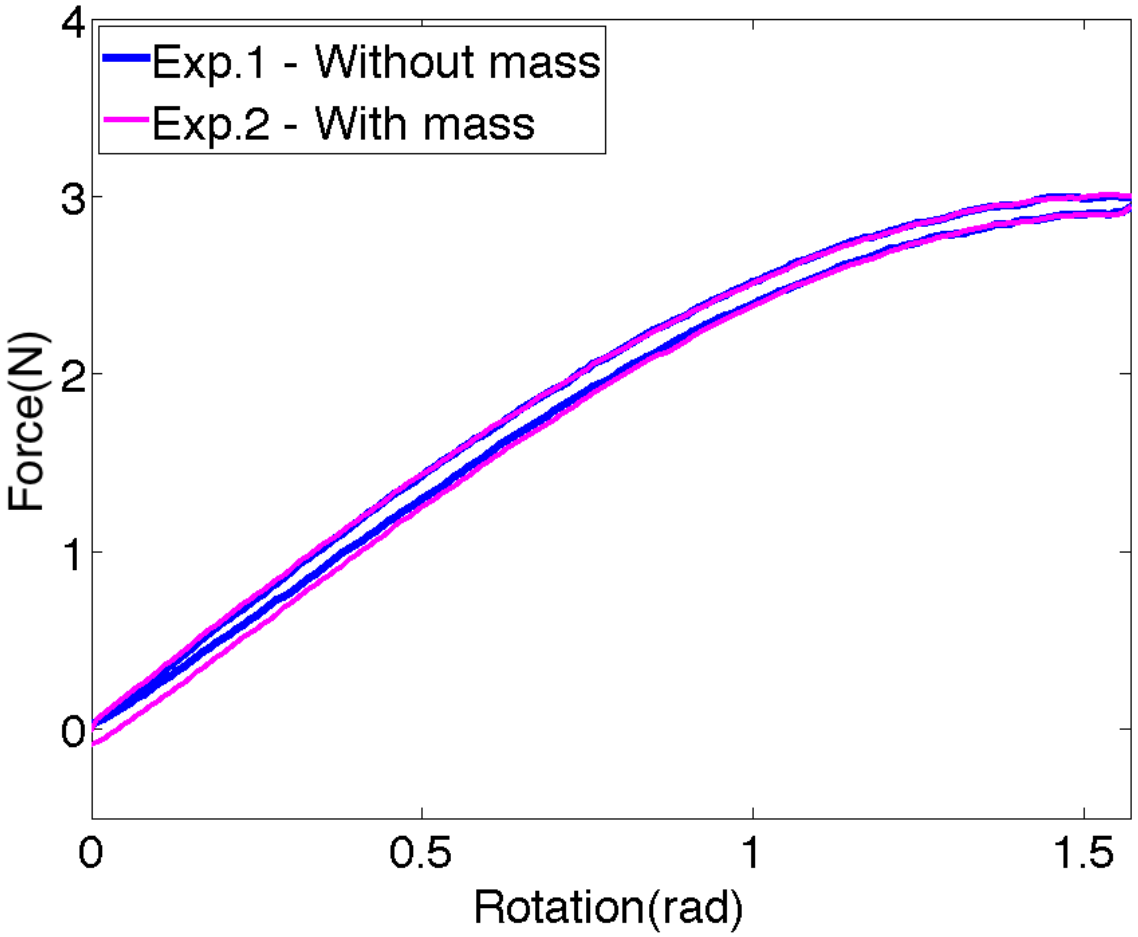

Figure G-3: Force-rotation characteristic of the unbalanced arm with(pink) and without an extra mass(blue).

Fig. G-4 shows the data of the experiments with one beam at the front (Exp. 3) and one beam at the back (Exp. 4) of the "arm". It can be concluded that the position of the beam did not have a large influence on the data. This implicates that the prototype was made symmetric.

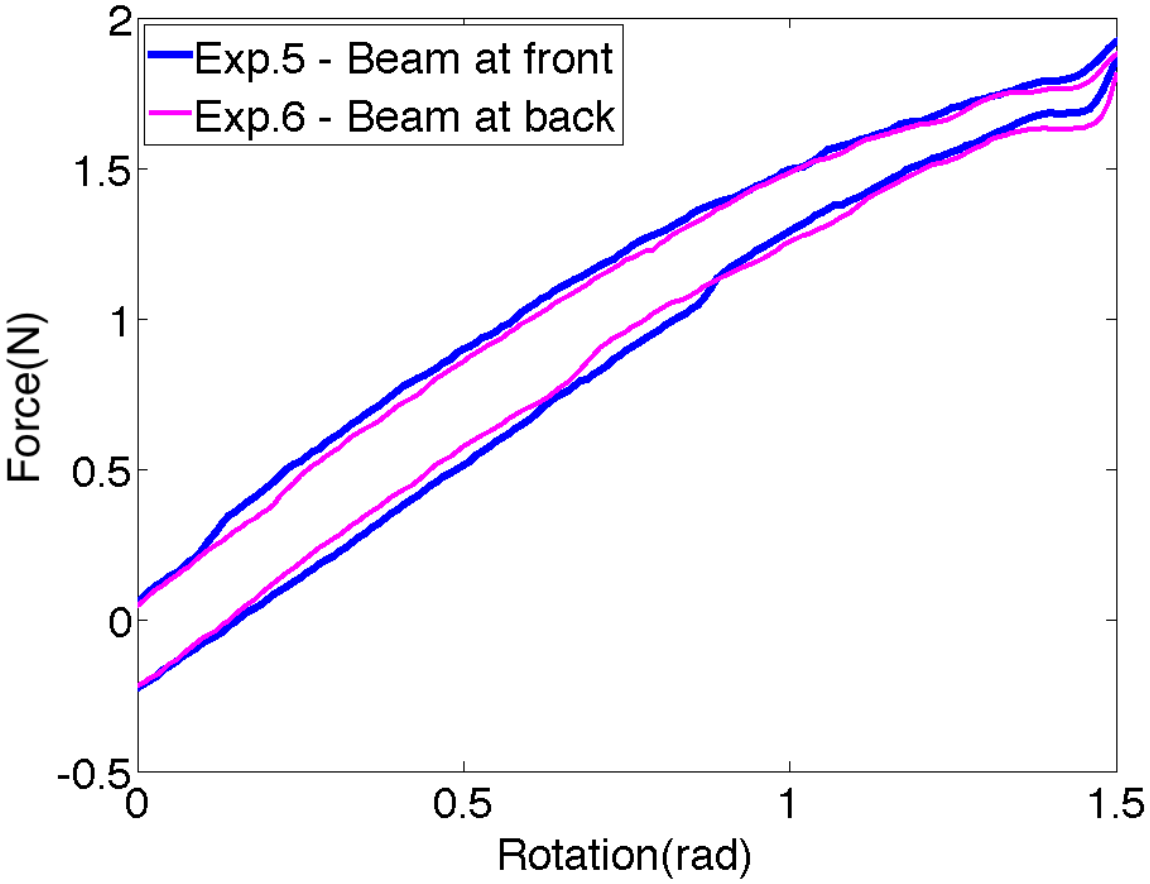

Figure G-4: Force-rotation characteristic of the experiment with one beam at the front(blue) and one beam at the back(pink).

Fig. G-5 shows the data of the experiments with two beams; with the extra mass (Exp. 5) and without the extra mass (Exp. 6). It is shown that at 0.75 rad the rotation of the "arm" stops and does not go back to its start position. This shows exactly the purpose of the mass; ensuring that the "arm" rotates back to its initial position.

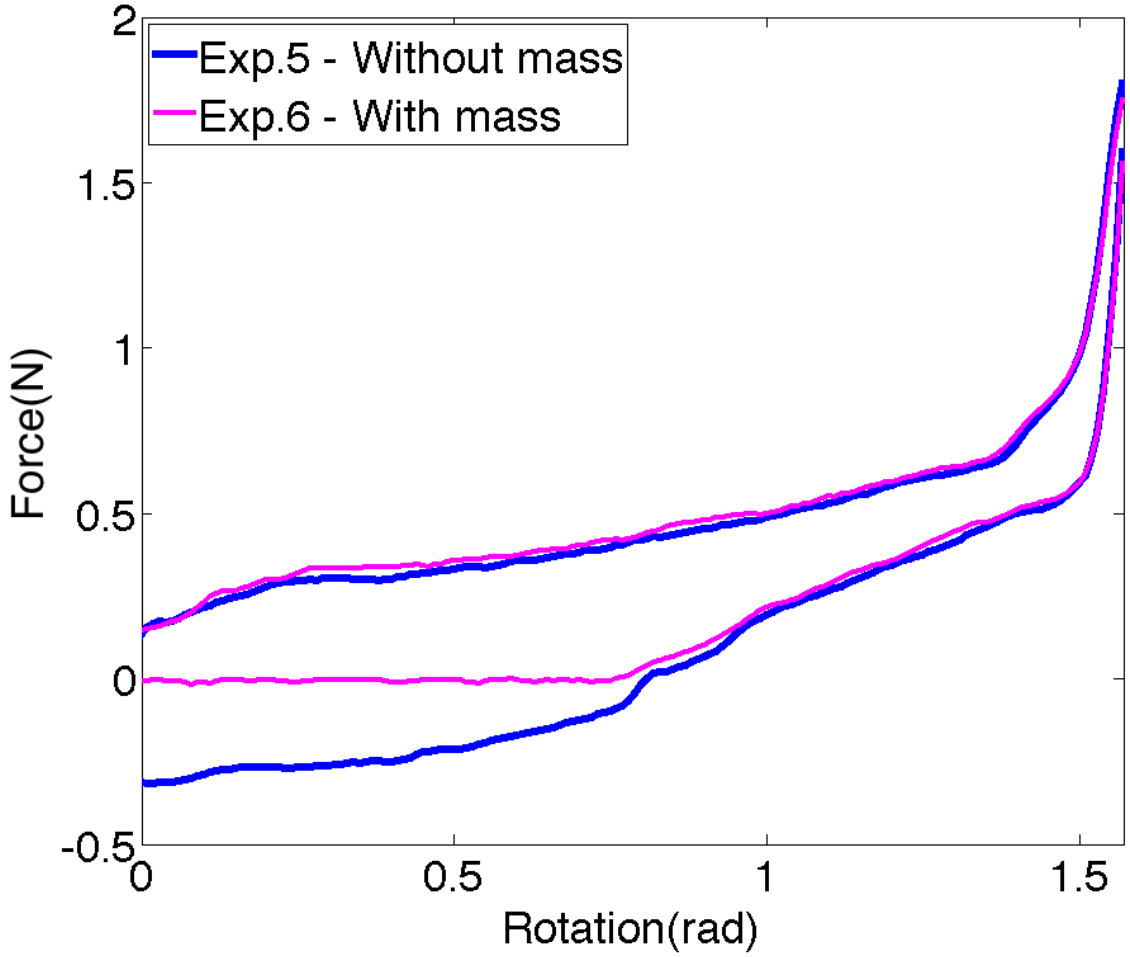

Figure G-5: Force-rotation characteristic of the experiments with two beams and an extra mass(blue) and without an extra mass(pink).

Fig. G-6 shows the data of the experiments with the same conditions(Exp. 6 and Exp. 7). It can be concluded that not a large variety exists among measurements with the same conditions.

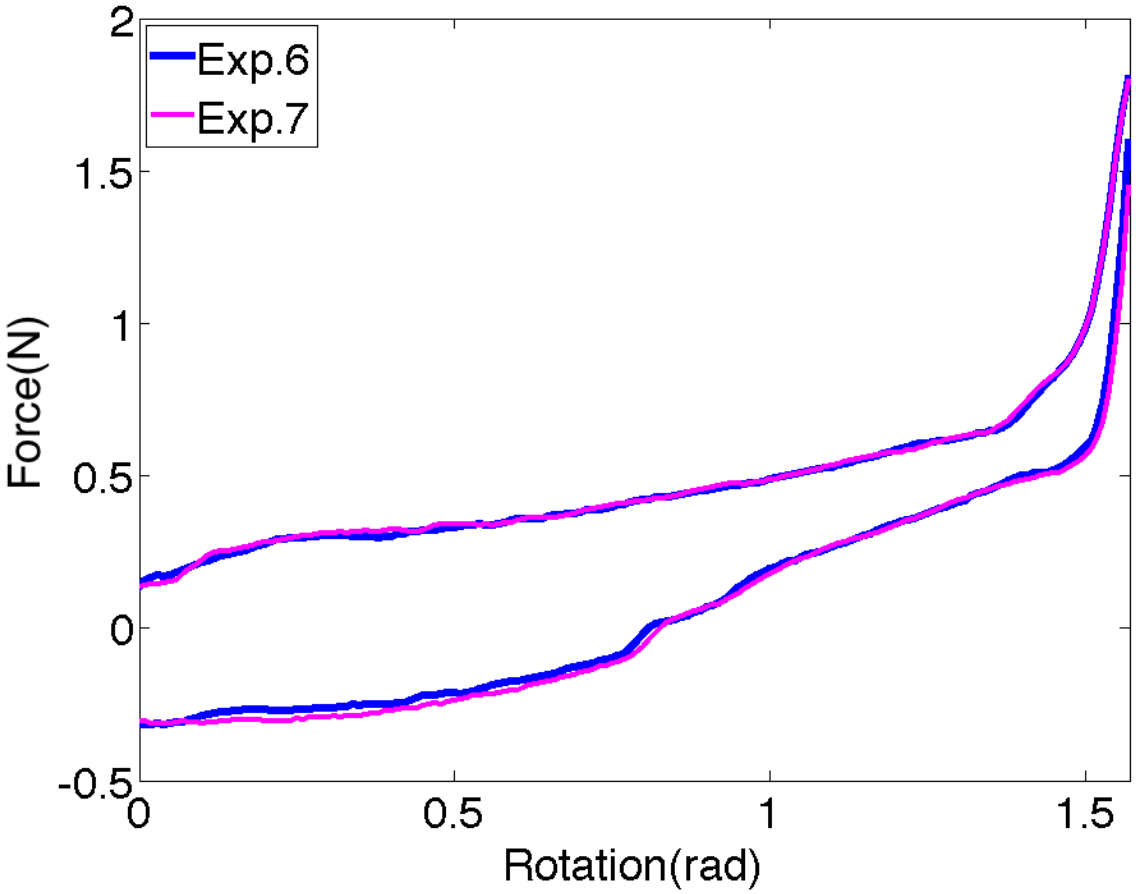

Figure G-6: Force-rotation characteristic of the experiments with two beams(Exp. 6 and Exp. 7)

Fig. G-7 shows the data of the experiments with beams of 0.7mm thickness (Exp. 7) and 0.8mm thickness (Exp. 8). It was expected that beams with 0.8mm thickness were able to store $(0.8/0.7)\hat{3}$=1.49 times less energy than beams of 0.7mm thickness while having the same width. Therefore the beams of 0.7mm thickness were made 1.49 times wider to have the same balancing capacity as the thicker beams. However, Fig. X shows that the thinner beams balances less good. The reason for this is not clear.

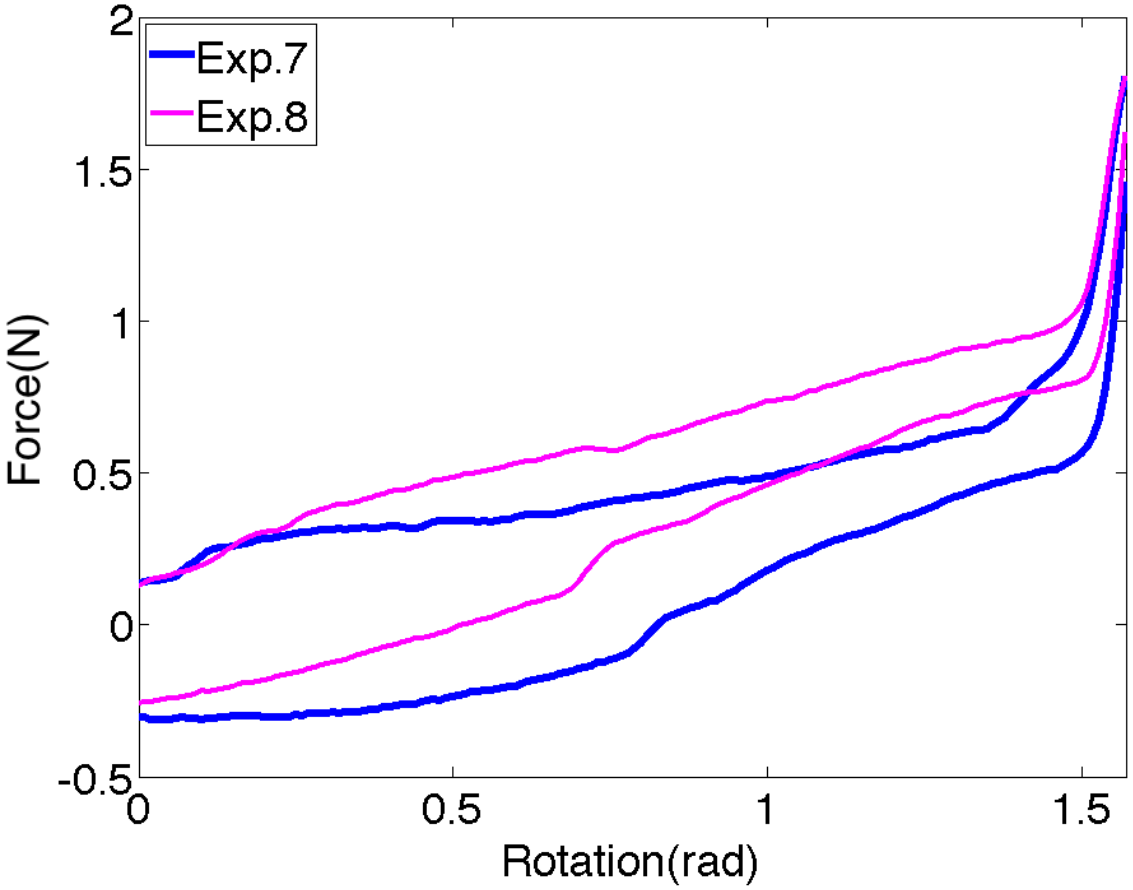

Figure G-7: Force-rotation characteristic of the experiments with beams of 0.7mm thickness(pink) and 0.8mm thickness(blue)

G-1 Difference in balancing force between up and down movement

The difference between the movement up and down of Fig. G-3 (without beams) is due to the friction between rod 1 and the socket. The experiments with beams do have a larger force difference between the up and down movement than the experiments without beams. This is because three extra sliding interfaces are added to the system, namely the friction between the screw and the socket, between the screw and the beam and between the beam and rod 2.

Appendix H

Prototype #2

H-1 Beams

H-1-1 Material

Pultruded carbon fibre square rods are used for the beams in this prototype. The fibre orientation is longitudinal and vinyl ester is used as matrix resin.

Table H-1 shows the results of tests with these rods performed by SKZ [12].

	Parameter	Unit	Material 1 (VEC™)	
			$\bar{x}$	s
4.1	Weight per meter	g/m	92.9	0.4
4.2	Flexural modulus of elasticity	GPa	108	1
	Flexural strength	MPa	835	37
	Elongation at flexural strength	%	0.78	0.03
4.3	Compression modulus of elasticity	GPa	71.0	8.3
	Compression stress at yield	MPa	483	48
	compressive strain at yield	%	2.0	0.2
4.4	Tensile modulus of elastic	GPa	133	12

Table H-1: Material properties of the CFRP-beams for prototype 2 [12]

H-1-2 Dimensions and balancing properties

The beams have a length of 0.232m to provide a range of motion from 0 to 1.57rad. Semi-finished beams were used with dimensions 0.0025x0.0025m. These beams provide a support of ś40% for an arm with a mass of 3.84kg(average men, age 18-30 [6]). Fig. H-1 shows a simulation of the moment that the prototype exerts on the arm.

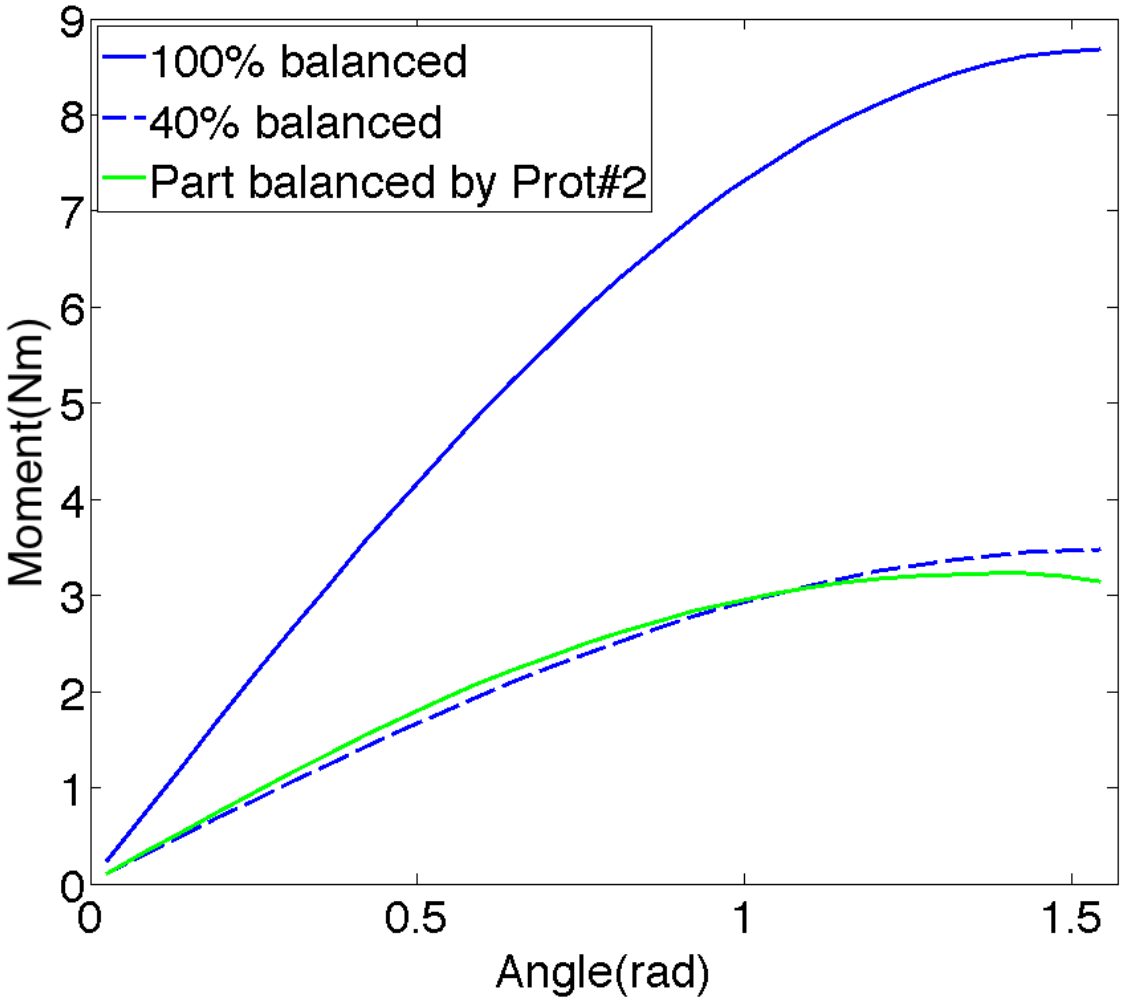

Figure H-1: Moment-angle characteristic of Prototype #2

H-2 Steel cable

Steel cable will be used with 0.45mm cross section, and minimum breaking load of 1770N/mm^2. This results in a breaking load of 282N for this wire. The maximum total force will be 134N, which is 33.5N per wire.

H-3 Fixation on environment

Options for fixing the construction to the environment.

Compliant joints

The rotational could be replaced by compliant joints. Advantages are that the compliant joints do not add friction to the system. Disadvantages are that it adds stiffness and the balancing capabilities will change. A small flexure will minimise the change of the balancing capabilities.

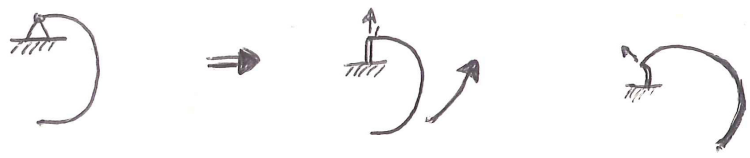

H-4 Photos of prototype #2

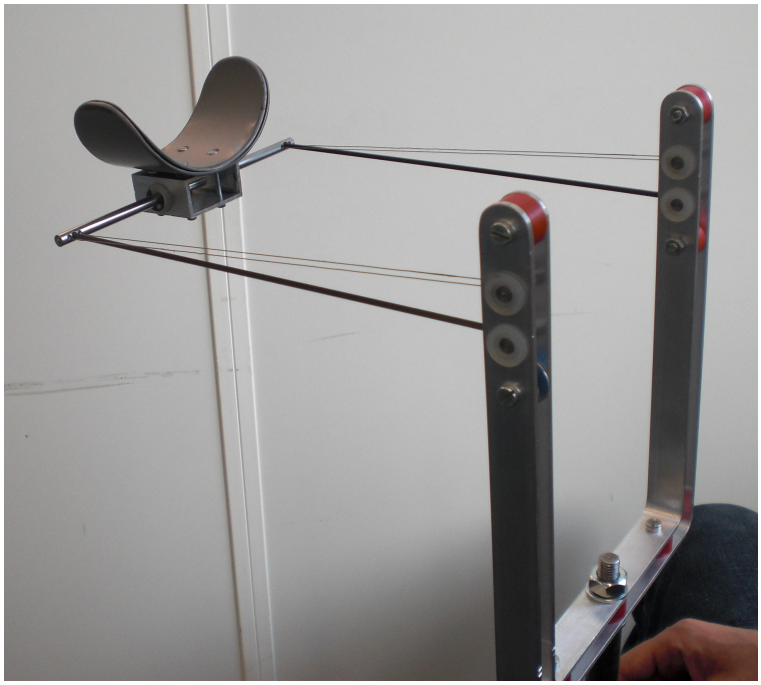

Figure H-2: Prototype #2, straight beams.

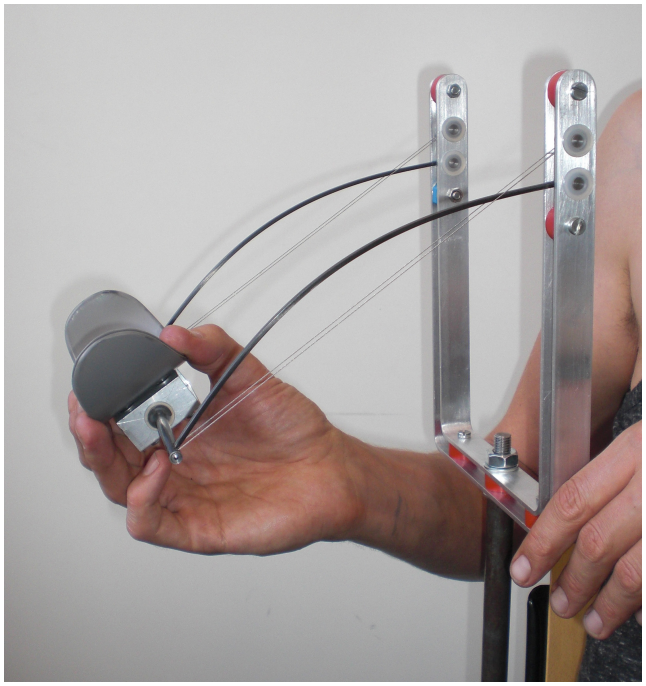

Figure H-3: Prototype #2, bended beams.

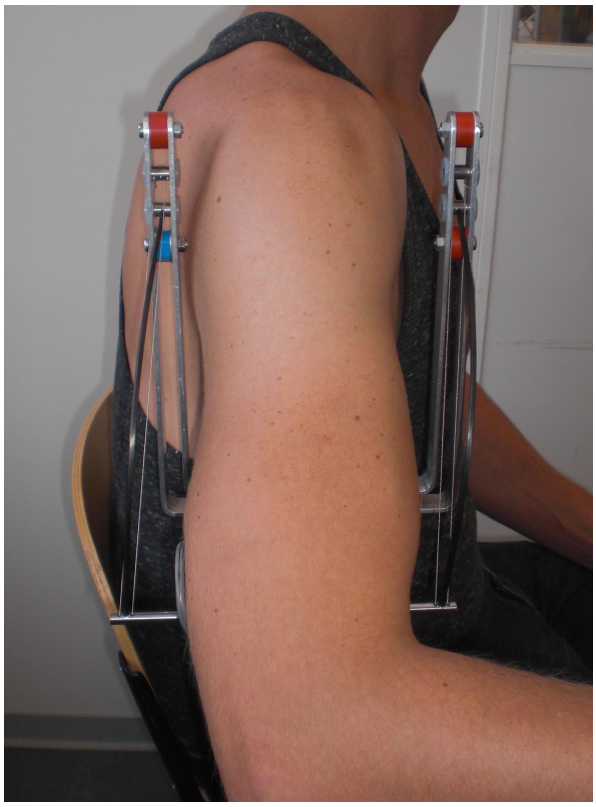

Figure H-4: Sideview of the prototype with arm.

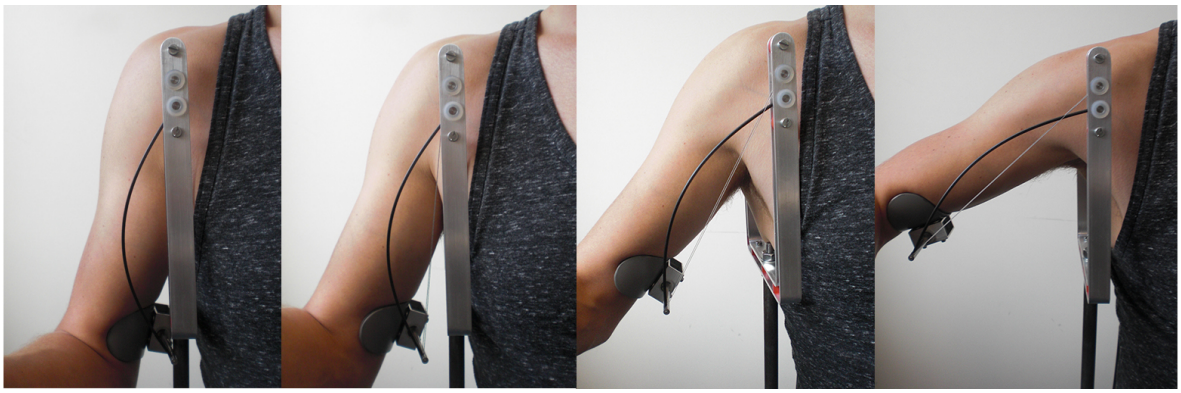

Figure H-5: Elevation of the arm with prototype #2.

Appendix I

Attachment to corset

This appendix shows the forces on the body and the corset if the beams and wires are attached to a corset.

I-1 Forces on corset

The following figures show free-body diagrams of the forces on the corset together with the equations and quantities.

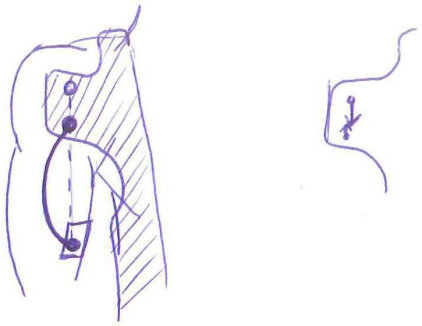

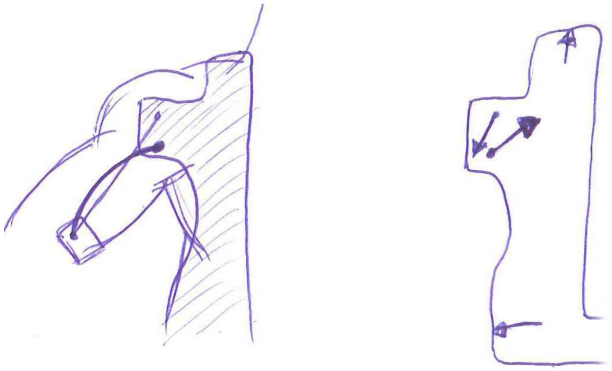

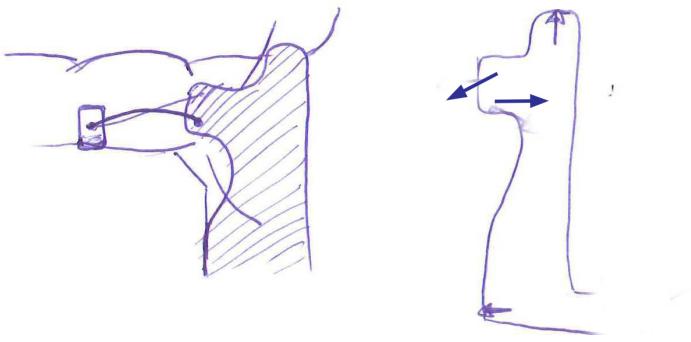

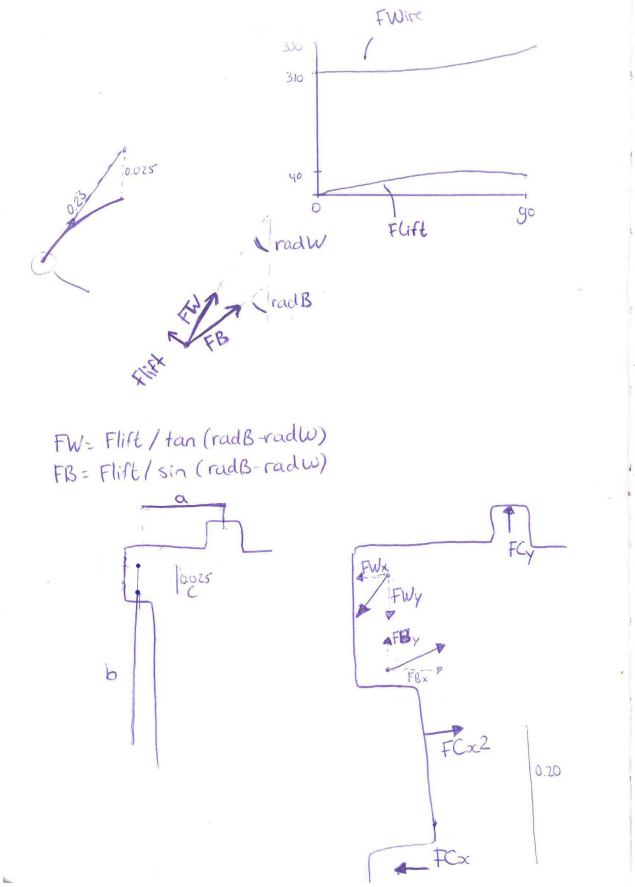

FW = Flift / tan (radB - radW)
FB = Flift / sin (radB - radW)

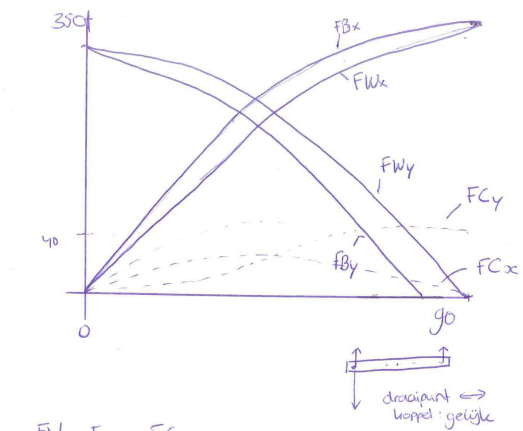

$FW_y - F_{By} = F_{Cy}$

$\sum_y (F_{By} + F_{Cy} - F_{Wy}) = 0$

$\sum_x (F_{Bx} - F_{(x} - F_{Wx}) = 0$
$+F_{Cx2}$

$\sum_M = F_{Cy} \cdot a + F_{Wx} \cdot b * - F_{Bx} \cdot (b - c) =$
0.05 0.025
om Fcx

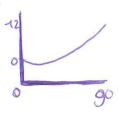

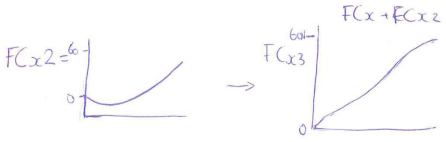

I-2 Forces on body

The following figure shows the forces on the body as a result of the forces on the corset and the device, with a distance d of 0.20m.

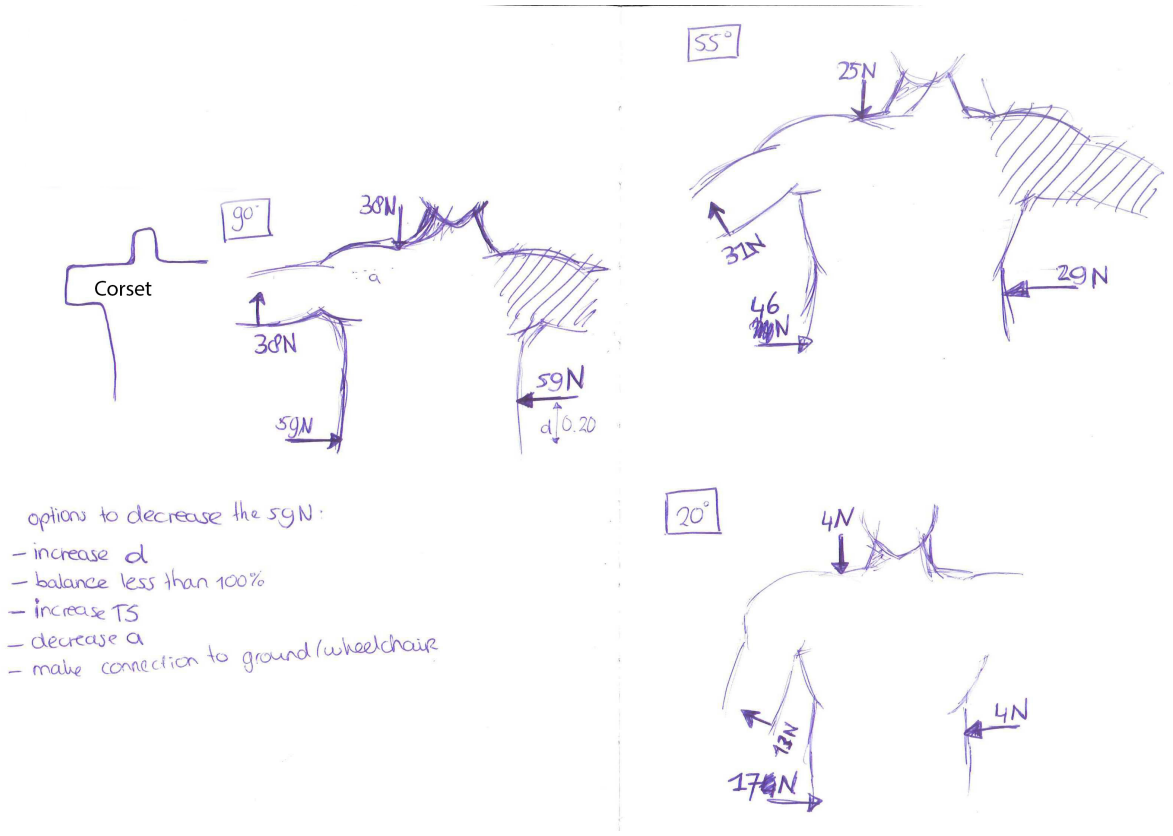

The distance d 0.20m, results in two forces at the waist. One force at the waist can suffice if b is larger. For a larger elevation of the arm, a larger distance b is required to make the system in equilibrium with one force at the waist.

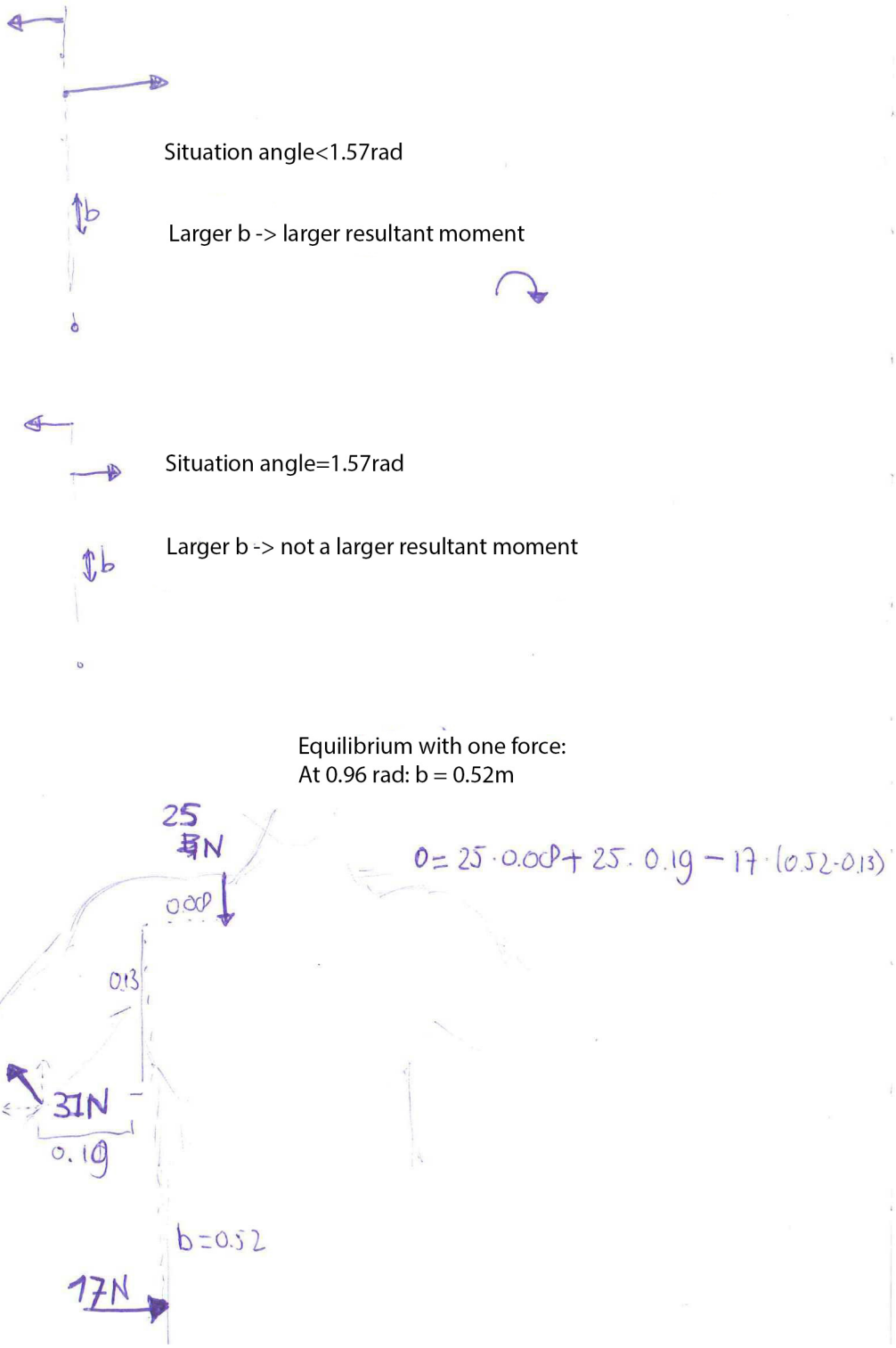

Appendix J

Forces at joints

J-1 Without beams

This function calculates the force of rod 1 on the socket during elevation without beams inserted.

```
% Fjoint without beams
m=0.540;g=9.81;radrot=0.20;CoM=0.105;rad=0:0.01:1.57;

% Calculation N (Force normal to "arm")
N=(CoM/radrot)*m*g*sin(rad);

% Calculation S (Force parallel to "arm")
r=63.6e-3; % radius circle
circ=2*pi*r; % circumference circle
perp=r/sqrt(0.20^2+r^2) % ratio Fwire : N
dirjoint=0.20/sqrt(0.20^2+r^2); % ratio Fwire : S
S=(dirjoint/perp)*N;

% Calculation Nx and Ny
Nx=N.*cos(rad);
Ny=N.*sin(rad);

% Calculation Sx and Sy
Sx=-S.*sin(rad);
Sy=S.*cos(rad);

% Calculation Cx and Cy (influence of rad)
W=(1/perp)*N; % Force in wire
Cx=-W-Sx-Nx;
Cy=-Sy-Ny;

% Calculation ICx and ICy (Total force in x and y direction)
```

```
ICx=Nx+Sx+Cx;
Fz=-m*g;
ICy=Ny+Sy+Fz+Cy;

% Calculation Fjoint
FjointW=sqrt(ICx.^2+ICy.^2);

%%
set(gca,'fontsize',35);set(gcf,'color','w');set(gcf,'Position', [0 100
    1000 800]);xlabel('Angle(rad)');ylabel('Force(N)')
plot(rad,ICx,rad,ICy,rad,FjointW,'LineWidth',4); hold on; legend('ICx','
    ICy','Rod 1','Location','NorthWest');axis([0 1.57 -10 15]);
```

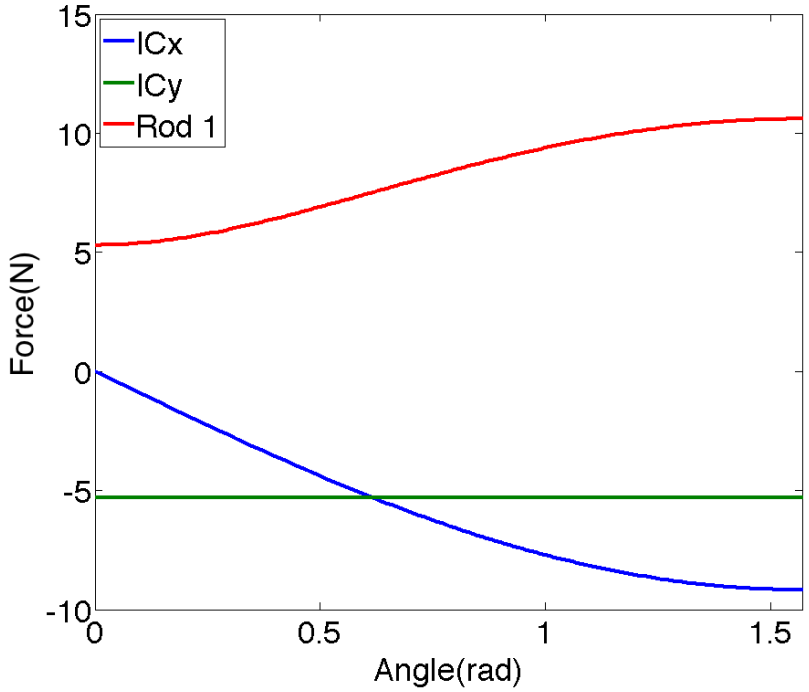

Figure J-1: Force of rod 1 on the socket in the x direction (ICx), y direction (ICy) and total (Fjoint).

J-2 With beams

This function calculates the sum of the forces between beams, socket, screws and rods.

```
%% Friction of beam
m=0.540;g=9.81;CoM=0.105;rad=0:0.01:1.57;

% Force N (Normal to arm)
radrot=0.20;
N=M2./radrot;% M2 is moment on arm

% Force B (Force of beam)
```

```
9  ICB1=0.025;% Distance between IC and B1
10 radW=rad;% Rad of wire
11 B1B2x=sin(radW)*radrot;% X - distance B2 to B1
12 B1B2y=cos(radW)*radrot-ICB1;% Y - distance B2 to B1
13 radB2=atan(B1B2x./B1B2y);
14 radB=radB2;
15 radB(146:end)=radB2(146:end)+1*pi;% Rad of beam
16 diffrad=radB-radW; % Angle between rad of beam and rad of wire
17 step=(1.57-1.57/38)/37;% 0.041315/2
18 Xint=(1.57/(38*2)):step:1.55;
19 M2int=interp1(Xint,M2,rad,'pchip');
20 F2int=M2int./radrot;
21 B=F2int./sin(diffrad); % Force of beam on joint
22
23 % Friction of beam not completed
24 Fcoef=0.4; % Coefficient of friction steel - acryl
25 FB=Fcoef*B;
26 r5=0.0025;% Radius hole
27 B1B2=B1B2x./sin(radB);
28 MB=(r5.*FB)./B1B2;
29
30 %% Friction of rod 1
31
32 % Calculation N (Force normal to "arm")
33 N=MWanted-M2;
34 Nint=interp1(Xint,M2,rad,'pchip');
35
36 % Calculation S (Force parallel to "arm")
37 r=63.6e-3; % radius circle
38 circ=2*pi*r; % circumference circle
39 perp=r/sqrt(0.20^2+r^2); % ratio Fwire : N
40 dirjoint=0.20/sqrt(0.20^2+r^2); % ratio Fwire : S
41 S=(dirjoint/perp)*Nint;
42
43 % Calculation Nx and Ny
44 Nx=Nint.*cos(rad);
45 Ny=Nint.*sin(rad);
46
47 % Calculation Sx and Sy
48 Sx=-S.*sin(rad);
49 Sy=S.*cos(rad);
50
51 % Calculation Bx and By
52 Bx=B.*sin(radB);
53 By=-B.*cos(radB);
54
55 plot(rad,Bx,rad,By)
56 legend('Bx','By')
57
58
59 % Calculation Cx and Cy (influence of rad)
60 W=(1/perp)*Nint; % Force in wire
61 Cx=-W-Sx-Nx;
```

```
62 Cy=-Sy-Ny;
63
64 plot(rad,Cx,rad,Cy)
65 legend('Cx','Cy')
66
67 % Calculation ICx and ICy (Total force in x and y direction)
68 ICx=Nx+Sx+Bx+Cx;
69 Fz=-m*g;
70 ICy=Ny+Sy+Fz+By+Cy;
71
72 % Calculation Fjoint
73 Fjoint=sqrt(ICx.^2+ICy.^2);
74
75 % Friction of rod1 not completed
76 Fcoef=0.4; % Coefficient of friction steel - acryl
77 FB=Fcoef*Fjoint;
78 M5=0.0025;% Radius hole
79 Mrod1=(M5/radrot).*FB;
80
81 %% Total force
82 TotalForce=2*B+Fjoint;
83 set(gca,'fontsize',35);set(gcf,'color','w');set(gcf,'Position', [0 100
       1000 800]);xlabel('Angle(rad)');ylabel('Force(N)')
84 plot(rad, B, rad,Fjoint,rad,TotalForce,'LineWidth',4); hold on; legend('
       Rod 1','B','Total');
85 axis([0 1.57 0 70])
```

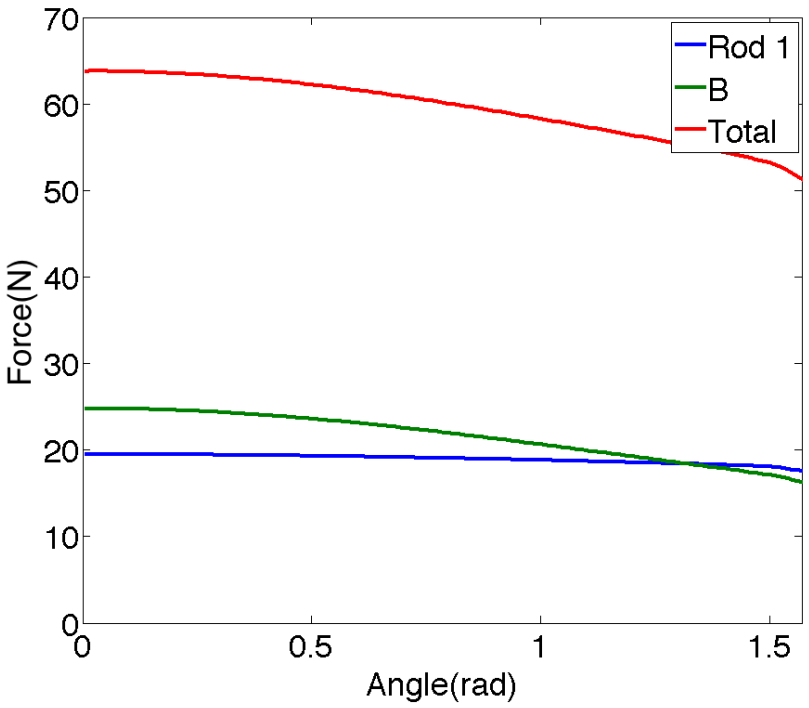

Figure J-2: Force of rod 1, the beams and the total forces ($Total = 2 * B + Rod1$).

Appendix K

Recommendations

Ideas for further development of the orthosis with bending beams:

- In the first place the focus was on the eating movement, but now the concept has to be extended to assist during other important daily activities. It was discovered that the arm of the first prototype can be balanced if a beam was connected to only one side of the socket. An orthosis that is only connected at the front of the shoulder, and not at the back, could have advantages such as an increased range of motion.
- Analysis of the stability properties of the orthosis with several configuration of the beams and for the case when degrees of freedom are added to the orthosis.
- Reconsider the configuration and amount of beams. It can be imagined that several beams with a smaller width can form a network that supports the arm even closer to the body.
- Incorporate balancing of the moment of the fore arm on the upper arm by extension of the orthosis to the fore arm.
- Analysis of the advantages of compliance in the orthosis. Explore if compliance result in an increased range of motion, without compromising on the support.

Bibliography

[1] J. Reswick and J. Rogers, "Experience at Rancho Los Amigos Hospital with devices and techniques to prevent pressure sores," *Bed sore biomechanics*, pp. 301–310, 1976.

[2] P. Brand, "Pressure sores - the problem," *Bed sore biomechanics*, pp. 19–23, 1976.

[3] C. J. van Andel, N. Wolterbeek, C. a. M. Doorenbosch, D. H. E. J. Veeger, and J. Harlaar, "Complete 3D kinematics of upper extremity functional tasks." *Gait & posture*, vol. 27, no. 1, pp. 120–7, Jan. 2008.

[4] A. Bergsma, "Design of a wearable arm support with passive gravity compensation," Tech. Rep., 2009.

[5] H.-I. Ma, W.-J. Hwang, P.-L. Tsai, and Y.-W. Hsu, "The effect of eating utensil weight on functional arm movement in people with Parkinson's disease: a controlled clinical trial." *Clinical rehabilitation*, vol. 23, no. 12, pp. 1086–92, Dec. 2009.

[6] *Dined, dined.io.tudelft.nl/dined/nl/.*

[7] D. A. Winter, *Biomechanics and motor conrol of human movement*, 4th ed. John Wiley & Sons, inc., 2009.

[8] *Sandvik, www.smt.sandvik.com.*

[9] *Diversified Structural Composites, www.diversified-composites.com.*

[10] *Hexcel, www.hexcel.com/Resources/Cont-Carbon-Fiber-Data-Sheets.*

[11] *Hasberg, www.hasberg-schneider.de/en/precision-thickness-gauge-strip-technical-info.html.*

[12] Das Kunststoff-Zentrum, "Comperative tests on CRP-profile with epoxy and vinyl ester matrix," 2012.